

LOCKHEED MISSILES & SPACE COMPANY
HUNTSVILLE RESEARCH & ENGINEERING CENTER
HUNTSVILLE RESEARCH PARK
4800 BRADFORD DRIVE, HUNTSVILLE, ALABAMA

ANALYSIS OF THE TRAJECTORY,
LOADS AND HEATING EXPERIENCED
BY A BODY PASSING THROUGH A
SUPERSONIC FLOW FIELD

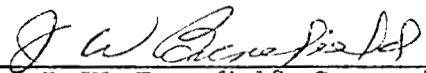
March 1967

Contract JPL-951567


by

R. J. Prozan
H. W. Butler

**This work was performed for the Jet Propulsion Laboratory,
California Institute of Technology, sponsored by the
National Aeronautics and Space Administration under
Contract NAS7-100.**

APPROVED BY: 
J. W. Benefield, Supervisor
Aero-Physics Section


D. C. Shea, Manager
Aero-Mechanics Department


J. S. Farrior
Resident Manager

FOREWORD

This document has been prepared by Lockheed Missiles & Space Company at its Huntsville Research & Engineering Center in conformance with the Statement of Work defined by Contract No. JPL-951567 issued by the California Institute of Technology, Jet Propulsion Laboratory. This contract is a sub-contract under NASA Contract NAS7-100 (Task Order No. RD-38).

This is the first of two documents concerning the work performed under Task II of the subject contract. The analytical effort is described here while the second document gives a detailed description of the computer program which was written to perform the necessary calculations.

ACKNOWLEDGEMENTS

The authors wish to acknowledge the contributions of the following LMSC/HREC personnel in the preparation of this document

- J. O. Golden for the Bray freezing discussion
- T. C. Davis for the free molecular loads discussion
- D. E. Kooker for the free molecular heating
- M. L. Blackledge for the continuum heating treatment
- K. R. Shrider for assisting in the program checkout.

SUMMARY

This document describes the analytical methods used to determine trajectories, loads and heating experienced by a spacecraft passing through a rocket exhaust field. Depending on body size and position in the exhaust, the spacecraft may be in free molecular, transitional, or continuum regimes.

The important features of this analysis are:

- Six-degree-of-freedom trajectory analysis
- Body shape description capable of handling complex unsymmetrical bodies
- Local wall pressures are defined over the entire vehicle
- Local heating rates are defined over the entire vehicle for the free molecule regime and the stagnation line for the continuum regime. Engineering approximations are employed for the off-stagnation line continuum regime and the transitional regimes.
- Flow regimes treated are continuum, transitional and free molecular
- Equilibrium/frozen thermochemistry for continuum plume description

The computer program created under this contract uses the thermochemical data generated by the NASA/Lewis Thermochemical program and communicates via magnetic tape with the output of the LMSC/HREC method of characteristics program. The result is a sophisticated, flexible, fully automated analysis of the effects on a spacecraft in a rocket exhaust environment. These features of the analysis are discussed generally within the body of this report. Detailed coverage of each of the main features is presented in Appendixes A through E.

CONTENTS

| Section | | Page |
|----------|--|------|
| | FOREWORD | ii |
| | SUMMARY | iii |
| 1 | INTRODUCTION | 1 |
| 2 | TECHNICAL DISCUSSION | 2 |
| | 2.1 Thermochemical Analysis and Freezing Criterion | 2 |
| | 2.2 Motion and Description of Immersed Vehicle | 4 |
| | 2.3 Flow Regimes | 5 |
| 3 | CONCLUSIONS AND FUTURE WORK | 9 |
| 4 | REFERENCES | 10 |
| Appendix | | |
| A | BRAY FREEZING CRITERION | A-1 |
| | A.1 Introduction | A-1 |
| | A.2 Freeze Point Determination | A-2 |
| | A.3 Discussion | A-6 |
| B | MOTION AND DESCRIPTION OF IMMERSSED VEHICLE | B-1 |
| | B.1 Introduction | B-1 |
| | B.2 Trajectory Calculation | B-3 |
| | B.3 Surface Geometry | B-8 |
| | B.4 Relative Velocity | B-13 |

CONTENTS (Continued)

| Appendix | | Page |
|----------|---|------|
| C | FREE MOLECULAR AND TRANSITIONAL FORCES | C-1 |
| | C.1 Forces Produced in Free Molecular Flow | C-1 |
| | C.2 Transition Flow Aerodynamic Characteristics | C-7 |
| D | FREE MOLECULAR HEATING | D-1 |
| | D.1 General Discussion | D-1 |
| | D.2 Front Side Heating | D-4 |
| | D.3 Back Side Heating | D-13 |
| E | CONVECTIVE HEATING | E-1 |
| | E.1 Method of Approach | E-1 |
| | E.2 Stagnation Point Heating Rate Solution | E-1 |
| | E.3 Windward Streamline Heating Distribution | E-2 |
| | E.4 Order of Solution | E-4 |
| | E.5 Start Conditions | E-8 |
| | E.6 Cylinder and Cone Integrations | E-8 |
| | E.7 Discontinuities | E-9 |
| | E.8 Local Properties | E-9 |
| | E.9 Off-Windward Streamline Distribution | E-10 |
| | E.10 Separation | E-10 |
| | E.11 Conclusions | E-11 |

Section 1 INTRODUCTION

A rocket exhaust plume constitutes an environment that is almost sure to have an adverse effect on any material surface which is exposed to it. If the surface in question is a spacecraft or a spacecraft component, precise knowledge of the environment and its effects becomes an important consideration in design and analysis. Heat transfer to exposed surfaces can create considerable problems on thin-skinned vehicles or temperature-sensitive components.

Another important aspect of the problem concerns spacecraft motion induced by the impinging gases. Rotational motions such as tumbling are highly undesirable. In general, induced rectilinear motion does not create as severe a problem although precise knowledge of the perturbations is still necessary before critical maneuvers such as rendezvous, reentry and earth-lunar transit can be attempted.

In this report, the general engineering and scientific concepts of a computer program which analyzes the impingement problems are presented. As an aggregate, the impingement solution presented here reflects state-of-the-art capabilities. A second report to be published approaches the problem from a computer programmer standpoint and describes each subroutine and its place in the overall calculation and contains input and output guides, as well as a sample problem.

This report is organized in such a manner that an appreciation of basic concepts, problems and method of solution can be obtained from the main body, while detailed discussion of the contributing disciplines can be found in the appendixes.

Section 2

TECHNICAL DISCUSSION

An accurate prediction of the impingement effects of a rocket plume involves the treatment of many scientific disciplines. The main features of such a calculation are:

- description of the thermochemical behavior of the propellants
- prediction of the undisturbed exhaust properties by gas dynamic and thermochemical methods
- vehicular motion and geometrical description
- calculation of body pressures and heat rates under various flow regimes

The thermochemical properties determination is made with the NASA/Lewis Thermochemical Program (Reference 1) while the flow field is described by the LMSC/HREC method-of-characteristics program of References 2, 3, and 4.

Following is a brief discussion of each of the disciplines employed to create an integrated computer program capable of providing the calculations required for this study.

2.1 THERMOCHEMICAL ANALYSIS AND FREEZING CRITERION

An accurate knowledge of impingement effects must necessarily begin with a prediction of the rocket exhaust flowfield. Previously supplied to JPL under this contract is a method of characteristics solution computer program (References 1, 2 and 3) capable of providing that solution. The solution can handle any thermochemical system whose properties can be predicted without any a priori knowledge of the flowfield, i.e., ideal, equilibrium, frozen, equilibrium/frozen thermochemical systems. While an ideal gas solution presents

no particular problem, the equilibrium and frozen analyses involve inputting a considerable amount of thermochemical information to the flowfield computer program. These data are generated by a specially modified version of the NASA/Lewis Thermochemical program (Reference 1). LMSC/HREC made these modifications to the thermochemical program so that the data transmission problem is eliminated. This special version, however, does not contain a freezing criterion such that the equilibrium/frozen analysis is cumbersome.

Real nozzle flows do not fall exactly into any of the categories listed above. Finite rate reactions always exist to some degree in any real system. Unfortunately, to handle complex flows with reaction kinetics is not practical at this time. Limitations such as lack of kinetic rate data, large run times, and complex chemical systems preclude the use of a finite rate analysis as an engineering tool in most cases. Since the types of propellants and flowfield conditions may vary widely, some less exact but more economical means of predicting the thermochemical behavior must be used. The assumption of infinite reaction rates (equilibrium) is excellent in high temperature, low speed flow regimes, while the assumption of frozen flow or very low reaction rates is excellent in high speed, low temperature regimes. The best trade-off between accuracy and economy in analyzing the flow system-thermochemical analysis is to combine the features of both equilibrium and frozen assumptions and change from one to the other at a freezing point.

Since the NASA/Lewis program did not have this capability, a task was defined under this contract to provide it. Two types of freezing criterion are permitted: (a) freeze pressure, (b) Bray multicomponent freeze criterion.

2.1.1 Freeze Pressure

If some prior knowledge or desired freeze pressure is known, then this option may be utilized. HREC has in the past utilized a finite rate one-dimensional calculation and observed the pressure at which the dominant reactions ceased. This pressure was then used as the freezing criterion. This is probably the

more accurate of the two analyses but it has one unfortunate drawback. An equilibrium flowfield solution must first be run and a representative streamline must be chosen for a subsequent finite rate analysis.

2.1.2 Bray Criterion

The Bray multicomponent freeze analysis has been incorporated into the NASA/Lewis program. Basically, the Bray freezing criterion amounts to an examination of the finite reaction rates in conjunction with a one-dimensional flowfield solution in order to determine where the flow radically departs from equilibrium. A more detailed discussion of this method may be found in Appendix A.

2.2 MOTION AND DESCRIPTION OF IMMERSED VEHICLE

These two rather unrelated subjects are grouped under one heading principally due to the commonality of coordinate systems and techniques used in the analysis. It is assumed that the vehicle may be described by an arrangement of three different shapes:

1. conic section of revolution
2. rectangular flat plate
3. circular flat plate or annulus

The conic section description is more powerful than it appears at first glance. In addition to those surfaces which are generally considered to be conic sections of revolution, cylinders, cones and frustums may be handled.

The arrangement of shapes can be such that the vehicle can be either symmetrical or nonsymmetrical and can be as simple as a sphere or as geometrically complicated as a deep space probe. A vehicle coordinate system is developed along the principal axis system. Various subshapes are then specified by type and coefficients. These subshapes are then related to the vehicle or composite system by transformations which are invariant with time.

The composite system is then related to the exit plane or thruster coordinate system. Of course, if the vehicle is in free flight, the thrusting system will be accelerating with respect to the composite system even without impingement loads. Although the exhaust itself is considered axisymmetric, there is no guarantee that the vehicle will not enter the exhaust at a skewed angle.

A six-degree-of-freedom trajectory program has been provided to calculate the vehicle motion. This solution uses a straightforward integration in time. This is certainly adequate, since the exposure time in the plume will generally be small. Gravitational and inertial rotating coordinate system effects have been neglected for the same reasons.

Impingement loads are calculated and referenced to the composite system origin and the next trajectory integration is performed. Initial data such as the vehicle shape, thrust of the exhausting vehicle and initial trajectory point is required.

For a more detailed discussion of the subjects treated in this section, See Appendix B.

2.3 FLOW REGIMES

As the vehicle passes through the exhaust, it may experience exhaust gases which vary from extremely dense to extremely rarefied. Of necessity, then, the impingement loads and heating analysis must be applicable in the continuum, transitional and free molecular flow regimes. These regimes are related to the ratio of number of intermolecular collisions to the number of surface collisions. This ratio is very high in the continuum regime and very low in the transitional regime. A commonly used method of deciding which flow regime is appropriate is to examine the Knudsen number;

$$\text{Knudsen number} = \frac{\text{mean free path}}{\text{reference length}}$$

While the Knudsen number which defines the various flow regimes is rather arbitrary, the most commonly accepted values are:

$$\begin{array}{rcl} & \left\{ \begin{array}{c} \\ \\ \end{array} \right. \text{Kn} & \begin{array}{l} \leq .01 \\ < 10 \\ > 10 \end{array} \end{array} \quad \begin{array}{l} \text{continuum} \\ \text{transitional} \\ \text{free molecular} \end{array}$$

The reference length used in the analysis is taken to be:

$$\text{reference length} = R_N \cos\theta + R_L \sin\theta$$

where R_N is the vehicle length normal to the minimum moment of inertia axis and R_L is the length parallel to that axis while θ is the angle of attack.

Having discussed the trajectory solution, the problems associated with developing the local pressures, hence the vehicle loads which will induce the motion, must now be investigated.

2.3.1 Free Molecular Flow

When the number of intermolecular collisions is small ($Kn > 10$) compared to the number of surface-molecule interactions, the surface is considered to be in free molecular flow. It is a reasonable assumption in the regime to treat the molecules with a Maxwellian velocity distribution. Since the impingement analysis of Section 2.2 will break each subshape into elemental areas, only the effect of a free molecular flow impinging on a flat plate need be considered.

Having assumed complete momentum and energy accommodation as well as diffuse reflection, Appendix C derives the equations necessary to calculate the pressure (more properly, force per unit area) in this regime.

The assumptions necessary to prescribe the free molecular heat rate are similar and are discussed in Appendix D.

2.3.2 Continuum Flow

The assumption of a continuous medium becomes valid for small Knudsen numbers. Because of the intermolecular collisions, boundary conditions or disturbances can make themselves felt in remote regions of the flow. Because of this, the analysis of loads and particularly heat rates becomes more complicated than in free molecular flow.

2.3.2.1 Continuum Surface Pressure Determination

For rocket exhaust flow fields the exit Mach number and hence the Mach number incident on the vehicle will always be high enough that Newtonian flow assumptions are valid.

The Newtonian flow assumption commonly used to predict the pressure distribution on a surface is

$$p_w = p_\infty (1 + \gamma M_\infty^2 \sin^2 \theta)$$

Another state property is needed, however, to unambiguously specify the gas properties on the wall. Since the above relation can be derived by assuming that the shock wave lies parallel to the wave, the same assumption can be used to obtain the other state variable.

2.3.2.2 Continuum Heating Analysis

The generality of a convective heating analysis for an arbitrary body immersed in a rocket exhaust plume is severely restricted by the necessity of predicting the growth of the viscous boundary layer as it flows over the body. This boundary layer growth is primarily a function of the body shape and of the magnitude and direction of the velocity of the surrounding flow-field with respect to the surface. These parameters must be uniquely specified for each particular body/flowfield configuration. In other words, a variation of the above parameters leads to different solutions of the governing equations, each of which is good only for the particular configuration and flowfield under analysis.

The following assumptions and the restricted list of body shapes are used when heating rates are estimated with the convective heating analysis discussed in Appendix E.

- The body must be an axisymmetric shape, i.e., a combination of cylinders or cone frustums with a pointed, blunted or hemispherically capped nosecone
- Heating rates off the stagnating streamline are adequately represented by an empirical correlation
- Real gas in chemical equilibrium exists throughout the flow-field
- Flow transition is assumed to occur as a step function based on momentum thickness Reynolds number
- The momentum thickness marching technique at compression and expansion corners is valid, or introduces only second-order errors
- Flow separation occurs on the vehicle on all surfaces which are shadowed from the approach flow
- Local convective heating rates are based on a constant input value of wall temperature, i.e., temperature of the wall is constant
- Local-to-stagnation point heating rate remains constant at a given body attitude in hypersonic flow

2.3.3 Transitional Flow

The transitional flow calculation is based on the theoretical values determined by free molecular flow and continuum flow theories. Since the pressures and heat rates experienced by the vehicle are known experimentally to vary smoothly from one regime to the other, it is possible to apply an empirical equation to predict the transitional value. This topic is discussed in Appendix C.

Section 3

CONCLUSIONS AND FUTURE WORK

In the preceding technical discussion a mathematical model and resultant computer program to describe the impingement effects of a jet exhaust on spacecraft motion was developed. Since the local Mach number found in a typical exhaust plume are generally sufficiently high for the Newtonian flow assumptions to be valid, the trajectory and continuum impingement loads calculations should give excellent results. In addition, free molecular flow theory for both heating and loads is well substantiated by experimental data. It is felt, therefore, that the foregoing analysis of these effects is entirely adequate for engineering application.

However, in the future the analysis could be improved when new analytical techniques and experimental data are found for the transition regime. State-of-the-art continuum heating analyses were beyond the scope of this effort but it is assumed that engineering prediction of heating rates in this flow regime could be improved by utilizing the more complex streamline divergence technique and, alternately, an entire three-dimensional viscous flow solution. The techniques necessary to achieve these improvements are now known for restricted body shapes.

Section 4
REFERENCES

1. Zeleznik, F. J. and S. Gordon, "A General IBM 7094 or 7090 Computer Program for Computation of Chemical Equilibrium Compositions, Rocket Performance and Chapman-Jouget Detonations," NASA TN D-1454, Lewis Research Center.
2. Prozan, R. J., "Development of a Method of Characteristics Solution for Supersonic Flow of an Ideal, Frozen or Equilibrium Reacting Gas Mixture," Technical Report, Lockheed Missiles & Space Company, Huntsville Research & Engineering Center, LMSC/HREC A783535, April 1966.
3. Ratliff, A. W., "Comparisons of Experimental Supersonic Flow Fields with Results Obtained by Using a Method of Characteristics Solution," Technical Report, Lockheed Missiles & Space Company, Huntsville Research & Engineering Center, LMSC/HREC A782592, April 1966.
4. Butler, H. W., "Description of a Digital Computer Program for Nozzle and Plume Analysis by the Method of Characteristics," Technical Report, Lockheed Missiles & Space Company, Huntsville Research & Engineering Center, LMSC/HREC A782592, December 1966.

APPENDIX A
BRAY FREEZING CRITERION

APPENDIX A NOMENCLATURE

| | |
|-----------------|--|
| a'_{ij} | stoichiometric coefficient for the i^{th} species in the j^{th} reaction |
| a''_{ij} | stoichiometric coefficient for the i^{th} species in the j^{th} reaction |
| k_f, k_r | rate constants in the forward and reverse direction |
| M_i | denotes species M_i , or molecular weight of species i |
| \bar{w} | average molecular weight |
| w_i | molecular weight of species i |
| t | time |
| V | velocity |
| X_i | mole fraction of species i |
| $a\{y-y_{eq}\}$ | defined by Equation (2) |
| ρ | density |
| $[\]$ | denotes concentration of a given specie |
| $_{eq}$ | subscript, denotes equilibrium value |
| y | nozzle axial distance |

BRAY FREEZING CRITERION

A.1 INTRODUCTION

In considering nozzle flow calculations for a multicomponent reacting system, the chemistry of the problem can be described by employing one of the following three assumptions.

- The flow is in local thermodynamic equilibrium at every point within the combustion chamber and the nozzle.
- The flow is in local thermodynamic equilibrium in the combustion chamber and is considered frozen at the combustion chamber composition at every point throughout the nozzle.
- The chemical reactions are allowed to proceed at a finite rate throughout the nozzle flow calculations with the rate of reaction controlled by the reaction kinetics of the system.

Nozzle flow calculations which incorporate either the equilibrium or frozen assumptions are relatively easy to handle. However, when either frozen or equilibrium chemistry is assumed throughout the nozzle flow, the proper description of the flow field and the correct performance parameters for the nozzle in question will not always be obtained. If the reaction rates for the reactions under consideration are very high, the local equilibrium assumption may yield reliable results. If the reaction rates are low, the frozen assumption may be satisfactory.

The most exact method of considering the chemistry problem in a multicomponent reacting system for nozzle flow calculations is to employ finite rate chemistry throughout the calculations. Although this method may yield the most

reliable flowfield calculations and nozzle performance parameters, there are several difficulties. First, a large amount of computer time may be required for the flow calculations. Second, reaction rate information may not be readily available or very reliable, thus negating the usefulness of the finite rate calculations.

One method to obtain rocket performance parameters approximating those obtained with finite rate calculations is to employ a sudden freezing criterion i.e., equilibrium chemistry is assumed up to a given nozzle point after which the flow is assumed chemically frozen. In many cases, this approach will provide useful results approaching the results of the finite rate calculations without excessive computer run time and the complexities of the finite rate chemistry nozzle flow calculations. Therefore, in response to the present study, a sudden freezing analysis was incorporated into an existing nozzle performance program. The freezing criterion was based upon the Bray Analysis (Reference A-1) and the nozzle performance code was the Lewis Thermochemical Program (References A-2 and A-3).

A.2 FREEZE POINT DETERMINATION

The Bray criterion is an approximate procedure for predicting where a reaction has departed significantly from equilibrium in a nozzle flow, i.e., determination of the freeze point. This prediction is made by determining the point at which the forward rate of reaction, r_f , becomes of the same order as the rate required to maintain equilibrium. Following the analysis given by Sarli, et al., Reference A-1, consider a nozzle expansion in which an arbitrary three-body reaction takes place.



The change of A_2 concentration with time at constant density is found from chemical kinetics to be

$$\left(\frac{\partial[A_2]}{\partial t}\right)_\rho = k_f [A_2][M] \left\{ \frac{[A]^2}{[A_2]} - \frac{[A]_{eq}^2}{[A_2]_{eq}} \right\} = a \{y - y_{eq}\} \quad (A.2)$$

The bracket, $[]$, in Equation (A.2) denotes the instantaneous concentration of the indicated species, k_f denotes the forward reaction rate constant and the subscript eq denotes instantaneous equilibrium values.

For near equilibrium flow $y - y_{eq} \ll y_{eq}$, and

$$\left(\frac{\partial[A_2]}{\partial t}\right)_\rho < < a y_{eq} \quad (A.3)$$

while for near frozen flow $y_{eq} \ll y$ and

$$\left(\frac{\partial[A_2]}{\partial t}\right)_\rho \simeq a y \gg a y_{eq} \quad (A.4)$$

Therefore, from Equations (A.3) and (A.4) it can be deduced that an approximate criterion for establishing the freezing point of the reaction is

$$\left(\frac{\partial[A_2]}{\partial t}\right)_\rho \simeq a y_{eq} = (r_f)_{eq} \quad (A.5)$$

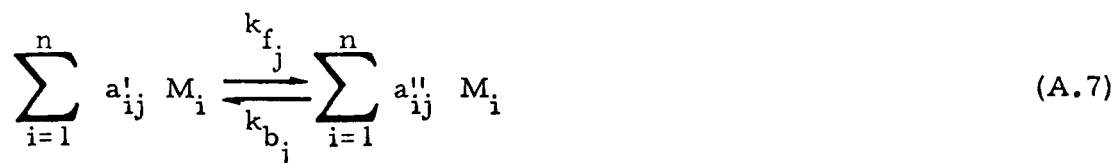
where r_f is evaluated with little loss in accuracy using equilibrium quantities up to the freezing point. The actual freezing point location is established by equating the forward reaction rate expressions, Equation (A.5), with the reaction

rate required to keep the particular species, A_2 , in equilibrium. This equilibrium reaction rate is given by the following expression.

$$\left(\frac{\partial [A_2]}{\partial t} \right)_{\rho, c_q} = \left[\frac{\rho V \partial \left(\frac{X_{A_2}}{\bar{w}} \right)}{\partial y} \right]_{eq} \quad (A.6)$$

where X_{A_2} is the mole fraction of A_2 and \bar{w} is the mean molecular weight of the gas.

The previous analysis was applied to a single reaction, however, the same line of reasoning may readily be applied to a multi-reaction system. The reactions may conveniently be written as in Reference A-4 for the j^{th} reaction.



where

a'_{ij} = stoichiometric coefficients of the i^{th} species in the j^{th} reaction for reactants

a''_{ij} = stoichiometric coefficients of the i^{th} species in the j^{th} reaction for the products

k_{fj}, k_{bj} = forward and reverse rate constants for the j^{th} reaction

M_i = i^{th} chemical species

The forward rate of reaction in terms of all reactions that make substantial contributions to the overall rate of production or depletion of species M_i is

$$\left(\frac{\partial [M_i]}{\partial t}\right)_\rho = \sum_{j=1}^N (a''_{ij} - a'_{ij}) \left\{ k_{fj} \prod_{k=1}^n [M_k]^{a'_{kj}} \right\} \quad (A.8)$$

where

N = total number of reactions

n = total number of species

From the equilibrium nozzle calculations, the reaction rate that is necessary to keep an important specie in equilibrium can be easily determined. The required time rate of change of the concentration of component i due to reaction is

$$\left(\frac{\partial [M_i]}{\partial t}\right)_{\rho, eq} = \left[\rho V \frac{d(X_i/\bar{w})}{dy} \right]_{eq} \quad (A.9)$$

where

X_i = mole fraction of species i

\bar{w} = mean molecular weight, $\bar{w} = \sum_{i=1}^n X_i w_i$

M_i = molecular weight of species i

Therefore, an effective freezing point for a multi-reaction system can be determined from Equations (A.8) and (A.9)

$$\begin{aligned} \left(\frac{\partial [M_i]}{\partial t}\right)_{\rho, eq} &= \left[\rho V \frac{d(X_i/\bar{w})}{dy} \right] = \left(\frac{\partial [M_i]}{\partial t}\right)_\rho \\ &= \sum_{j=1}^N (a''_{ij} - a'_{ij}) \left\{ k_{fj} \prod_{k=1}^n [M_K]^{a'_{kj}} \right\} \end{aligned} \quad (A.10)$$

From the above relations, it is clear that there may be as many freezing points as there are atoms or radicals to which Equation (A.10) is applied. However, these freezing points are usually in close proximity to one another, depending on the choice of reactions employed in the forward reaction rate equation.

A.3 DISCUSSION

Caution is in order when applying the single reaction Bray freezing point criterion. Its use is really justified only after extensive evaluation of the kinetics of the system have been made using an exact kinetic flow model, and it has been established that a single reaction is rate controlling.

The composite reaction freezing point criterion (modified Bray composite reaction criterion) is, in general, more satisfactory than the single reaction criterion, although some prior knowledge of the kinetic behavior of the specific propellant system under consideration is needed for best results. The concept of a composite-reaction freezing point is based on the assumption that an important rate controlling species exists, whose net rate of formation or depletion becomes very small as the reactions in which it participates become very slow, and that once this species has frozen at some point in the nozzle, all remaining species no longer react. The problem of locating this "composite-reaction freezing point" then reduces to determining kinetically the important species and reactions which must be considered. Quite often, the importance of many of the species may be evaluated on the basis of:

- The equilibrium composition values
- The energy release of the chemical reactions in which they participate
- The role of the species in the overall reaction mechanism.

Sarli, et al., in their analysis of sudden freezing criteria have noted several limitations of this technique. They suggest that the sudden freezing analysis is potentially inaccurate to a substantial degree when the freeze point is located near the vicinity of the nozzle throat. Further, they state that the dominant reaction or dominant species to be considered in the sudden freezing analysis for a particular propellant system may change as the O/F ratio changes or as the relative rates of the various recombination reactions are varied to account for uncertainties in the kinetic data.

From the previous analysis, it can be seen that employment of the sudden freezing criterion requires the following information:

- Equilibrium nozzle flow solution
- Reaction model for the propellant system in question
- Reaction rate data for reaction model used

Further, nozzle geometry information was required when the freezing analysis was incorporated into the Lewis Thermochemical code. The details of the code modification will be presented in the user's manual.

APPENDIX A REFERENCES

- A-1 Sarli, V. J., W. G. Burwell and R. Hofland, Jr., "Evaluation of the Bray Sudden-Freezing Criterion for Predicting Nonequilibrium Performance in Multi-reaction Rocket Nozzle Expansions," AIAA Propulsion Joint Specialist Conference, Paper No. 65-554, Colorado Springs, Colorado, 14 - 18 June 1965.
- A-2 Zeleznik, F. J. and Sanford Gordon, "A General IBM 704 or 7090 Computer Program for Computation of Chemical Equilibrium Compositions, Rocket Performance and Chapman-Jouget Detonations," NASA TN D-1454, October 1962.
- A-3 Gordon, Sanford and F. J. Zeleznik, "A General IBM 704 or 7090 Computer Program for Computation of Chemical Equilibrium Compositions, Rocket Performance and Chapman-Jouget Detonations, Supplement I - Assigned Area-Ratio Performance," NASA TN D-1737, October 1963.
- A-4 Penner, S. S., "Chemistry Problems in Jet Propulsion," Pergamon Press, MacMillian Company, New York, 1957.

APPENDIX B

MOTION AND DESCRIPTION OF IMMERSED VEHICLE

APPENDIX B NOMENCLATURE

| | |
|--|---|
| a, b, c, d, e | coefficients of surface equations |
| $c\omega_1, c\omega_2, c\omega_3$ | cosines of Eulerian angles |
| \overline{F} | force vector |
| $\overline{i}, \overline{j}, \overline{k}$ | unit vectors of coordinate system |
| \overline{n} | unit normal vector |
| \overline{P} | location of a point in space |
| \overline{R} | radius vector to a point in space |
| S | surface of composite structure |
| $s\omega_1, s\omega_2, s\omega_3$ | sines of Eulerian angles |
| $[T]$ | transfer matrix |
| \tilde{T} | torque vector |
| $[T]^T$ | transpose of transfer matrix |
| t | time |
| x, y, z | Cartesian coordinates |
| I | moments of inertia |
| <u>Greek Symbols</u> | |
| α, β, γ | angles of x, y, z axis with respect to reference axis |
| ξ | arbitrary vector |
| ν, ϕ | cylindrical coordinates |
| $\omega_1, \omega_2, \omega_3$ | Eulerian angles |
| θ | flow angle |

APPENDIX B NOMENCLATURE (Continued)

Subscripts

| | |
|----|--|
| b | base |
| C | composite structure axis system |
| CE | vector or transfer matrix from "C" to "E" system |
| CI | vector or transfer matrix from "C" to "I" system |
| E | exit plane axis system |
| EC | vector or transfer matrix from "E" to "C" system |
| F | flow |
| I | subshape axis system |
| IC | vector or transfer matrix from "I" to "C" system |
| n | nose |
| R | relative |
| T | nozzle throat axis system |

Superscripts

| | |
|-----|--------------------------|
| (0) | evaluated at time zero |
| + | evaluated at new time |
| . | velocity of quantity |
| .. | acceleration of quantity |

MOTION AND DESCRIPTION OF IMMERSED VEHICLE

B.1 INTRODUCTION

A rocket exhaust plume will have been calculated by the method of characteristics and stored on magnetic tape. Also on this tape will be a description of the thermochemical behavior of the gas system.

The exhaust gases may impinge on some surfaces in the plume and it is necessary to calculate the reaction forces, heating rates and resultant motion. It is assumed that the body or vehicle in question may be accurately represented by some composite arrangement of simple subshapes. Three such subshapes are

- conic section of revolution
- rectangular flat plate
- circular flat plate

Before discussing the impingement calculation and subsurface geometry it is in order to describe the basic coordinate systems and trajectory analysis to be used.

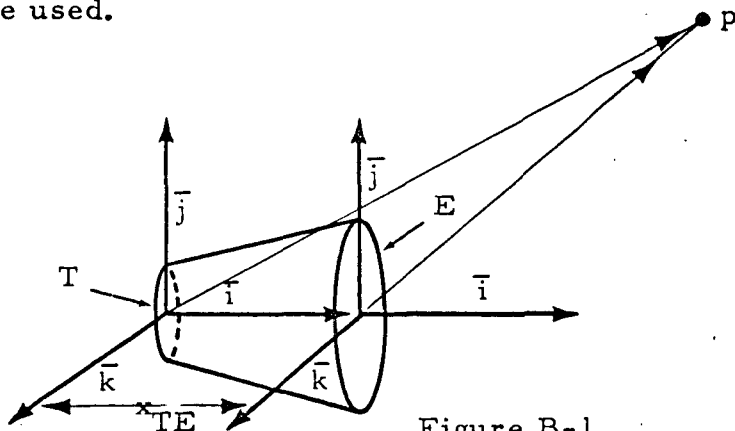


Figure B-1

Generally the flowfield calculation will be referenced to the nozzle throat while it is most desirable to locate the origin of coordinates at some other station, say the nozzle exit plane, so that, referring to Figure B-1

$$\bar{P} = \bar{P}_E + x_{TE} \bar{i}_E$$

Of course

$$\bar{i}_T = \bar{i}_E, \bar{j}_T = \bar{j}_E, \bar{k}_T = \bar{k}_E$$

Let the c.g. of the vehicle be the origin of coordinates for information pertaining to the vehicle. Let one of the axis be aligned along the principal minimum moment of inertia axis.

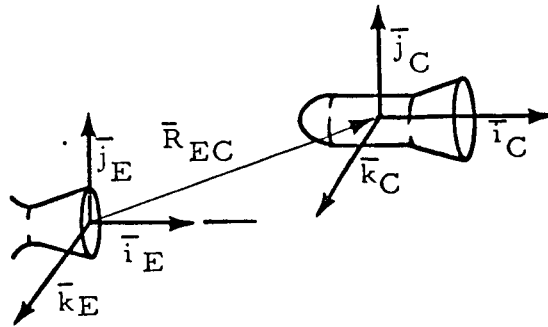


Figure B-2

At some time the position vector \bar{R}_{EC} (see Figure B-2) must be given at time zero, for instance;

$$\bar{R}_{EC}^{(0)} = x_{EC}^{(0)} \bar{i}_E + y_{EC}^{(0)} \bar{j}_E + z_{EC}^{(0)} \bar{k}_E = \begin{Bmatrix} x & y & z \end{Bmatrix}_{EC}^{(0)} \begin{Bmatrix} \bar{i} \\ \bar{j} \\ \bar{k} \end{Bmatrix}_E$$

while

$$\bar{i}_C^{(0)} = \cos \alpha_{ECi}^{(0)} \bar{i}_E + \cos \beta_{ECi}^{(0)} \bar{j}_E + \cos \gamma_{ECi}^{(0)} \bar{k}_E$$

If the body is not axisymmetric it is necessary to specify

$$\bar{j}_C^{(0)} = \begin{Bmatrix} \cos \alpha & \cos \beta & \cos \gamma \end{Bmatrix}_{ECj}^{(0)} \begin{Bmatrix} \bar{i} \\ \bar{j} \\ \bar{k} \end{Bmatrix}_E$$

while if the body is axisymmetric \bar{j}_C will be defined by

$$\frac{j_C^{(0)} = \left\{ \cos \gamma \cos \alpha \cos \beta \right\}_{ECi}^{(0)} \begin{Bmatrix} \bar{i} \\ \bar{j} \\ \bar{k} \end{Bmatrix}_E \times \left\{ \cos \alpha \cos \beta \cos \gamma \right\}_{ECi}^{(0)} \begin{Bmatrix} \bar{i} \\ \bar{j} \\ \bar{k} \end{Bmatrix}_E}{\text{mag (numerator)}}$$

This coordinate system for axisymmetric bodies simplifies the subsequent continuum heating analysis. The coordinate system definition is completed by

$$\bar{k}_C^{(0)} = \bar{i}_C^{(0)} \times \bar{j}_C^{(0)}$$

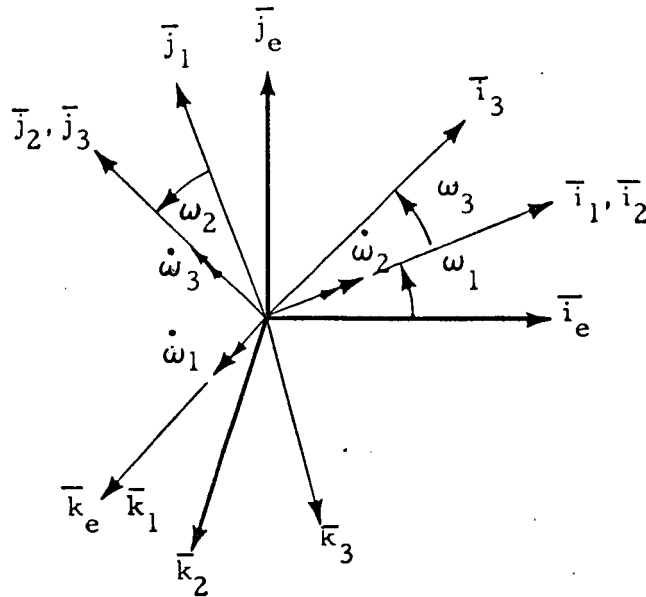
or

$$\begin{Bmatrix} \bar{i} \\ \bar{j} \\ \bar{k} \end{Bmatrix}_C^{(0)} = [T_{EC}]^{(0)} \begin{Bmatrix} \bar{i} \\ \bar{j} \\ \bar{k} \end{Bmatrix}_E$$

B.2 TRAJECTORY CALCULATION

The moments of inertia and mass of the composite body are given. It will be assumed that the axes are the principal axes. As the vehicle is exposed to exhaust gas impingement, it may be expected to rotate as well as translate. The trajectory program therefore will, of necessity, be a six-degree-of-freedom analysis.

It is first necessary to define the orientation of the composite shape coordinate system with respect to the nozzle exit system. Consider the Eulerian rotations shown on the following page.



where the order of rotation is $\omega_1, \omega_2, \omega_3$. Then

$$\begin{pmatrix} \bar{i} \\ \bar{j} \\ \bar{k} \end{pmatrix}_C = \begin{pmatrix} \bar{i} \\ \bar{j} \\ \bar{k} \end{pmatrix}_3 = \begin{bmatrix} 2^T C \end{bmatrix} \begin{bmatrix} 1^T 2 \end{bmatrix} \begin{bmatrix} E^T 1 \end{bmatrix} \begin{pmatrix} \bar{i} \\ \bar{j} \\ \bar{k} \end{pmatrix}_E$$

where

$$\begin{bmatrix} 2^T C \end{bmatrix} = \begin{bmatrix} c\omega_3 & 0 & -s\omega_3 \\ 0 & 1 & 0 \\ s\omega_3 & 0 & c\omega_3 \end{bmatrix}$$

$$\begin{bmatrix} 1^T 2 \end{bmatrix} = \begin{bmatrix} 1 & 0 & 0 \\ 0 & c\omega_2 & s\omega_2 \\ 0 & -s\omega_2 & c\omega_2 \end{bmatrix}$$

$$\begin{bmatrix} E^T 1 \end{bmatrix} = \begin{bmatrix} c\omega_1 & s\omega_1 & 0 \\ -s\omega_1 & c\omega_1 & 0 \\ 0 & 0 & 1 \end{bmatrix}$$

Because of the convention adopted at transformation is defined

$$\begin{pmatrix} \bar{i} \\ \bar{j} \\ \bar{k} \end{pmatrix} = [T] \begin{pmatrix} \bar{i} \\ \bar{j} \\ \bar{k} \end{pmatrix}$$

but a vector transforms

$$\{x' \ y' \ z'\} = \{x \ y \ z\} [T]^T$$

The angular velocity $\dot{\bar{\omega}}_C$ is

$$\dot{\bar{\omega}}_C = \begin{Bmatrix} \dot{\omega}_{Cx} & \dot{\omega}_{Cy} & \dot{\omega}_{Cz} \end{Bmatrix} \begin{pmatrix} \bar{i} \\ \bar{j} \\ \bar{k} \end{pmatrix}_C$$

but $\dot{\bar{\omega}}_C$ can also be written

$$\dot{\bar{\omega}}_C = \dot{\omega}_1 \bar{k}_E + \dot{\omega}_2 \bar{i}_1 + \dot{\omega}_3 \bar{j}_C$$

$$\dot{\bar{\omega}}_C = \left[\begin{Bmatrix} 0 & 0 & \dot{\omega}_1 \end{Bmatrix} [E^T C]^T + \begin{Bmatrix} \dot{\omega}_2 & 0 & 0 \end{Bmatrix} [1^T C]^T + \begin{Bmatrix} 0 & \dot{\omega}_3 & 0 \end{Bmatrix} \right] \begin{pmatrix} \bar{i} \\ \bar{j} \\ \bar{k} \end{pmatrix}_0 \quad (B.1)$$

where

$$[1^T C] = \begin{bmatrix} c\omega_3 & s\omega_2 s\omega_3 & -s\omega_3 c\omega_2 \\ 0 & c\omega_2 & s\omega_2 \\ s\omega_3 & -s\omega_2 c\omega_3 & c\omega_2 c\omega_3 \end{bmatrix}$$

$$[E^T C] = \begin{bmatrix} (c\omega_3 c\omega_1 - s\omega_1 s\omega_2 s\omega_3) & (c\omega_3 s\omega_1 + c\omega_1 s\omega_2 s\omega_3) & (-s\omega_3 c\omega_2) \\ (-c\omega_2 s\omega_1) & (c\omega_2 c\omega_1) & (s\omega_2) \\ (c\omega_1 s\omega_3 + s\omega_2 c\omega_3 s\omega_1) & (s\omega_3 s\omega_1 - c\omega_1 s\omega_2 s\omega_3) & (c\omega_2 c\omega_3) \end{bmatrix}$$

Equation (B.1) becomes

$$\dot{\bar{\omega}}_C = \left\{ (\dot{\omega}_2 c\omega_3 - \dot{\omega}_1 s\omega_3 c\omega_2) \quad (\dot{\omega}_3 + \dot{\omega}_1 s\omega_2) \quad (\dot{\omega}_2 s\omega_3 + \dot{\omega}_1 c\omega_2 c\omega_3) \right\} \begin{bmatrix} \bar{i} \\ \bar{j} \\ \bar{k} \end{bmatrix}_C$$

or

$$\dot{\omega}_{Cx} = \dot{\omega}_2 c\omega_3 - \dot{\omega}_1 s\omega_3 c\omega_2$$

$$\dot{\omega}_{Cy} = \dot{\omega}_3 + \dot{\omega}_1 s\omega_2$$

$$\dot{\omega}_{Cz} = \dot{\omega}_2 s\omega_3 + \dot{\omega}_1 c\omega_2 c\omega_3 \quad (B.2)$$

Now Euler's equations of motion for a principal axis system are

$$\ddot{\omega}_{Cx} = [T_x + (I_y - I_z) \dot{\omega}_{Cy} \dot{\omega}_{Cz}] / I_x$$

$$\ddot{\omega}_{Cy} = [T_y + (I_z - I_x) \dot{\omega}_{Cx} \dot{\omega}_{Cz}] / I_y$$

$$\ddot{\omega}_{Cz} = [Tz + (Ix - Iy) \dot{\omega}_{Cx} \dot{\omega}_{Cy}] / Iz$$

Integrating to the next time step yields

$$\dot{\omega}_C^+ = \dot{\omega}_C + \ddot{\omega}_C \Delta t$$

The inverse relation of Equation (B.2) is

$$\dot{\omega}_1^+ = (\dot{\omega}_{Cx}^+ s\omega_z - \dot{\omega}_{Cz}^+ c\omega_3) / c\omega_2$$

$$\dot{\omega}_2^+ = [\dot{\omega}_{Cx}^+ (1 + s\omega_2 s\omega_3) - \dot{\omega}_{Cz}^+ c\omega_3 s\omega_3] / c\omega_3$$

$$\dot{\omega}_3^+ = \dot{\omega}_{Cy}^+ - (\dot{\omega}_{Cx}^+ s\omega_2 + \dot{\omega}_{Cz}^+ c\omega_3) \frac{s\omega_3}{c\omega_2}$$

and integrating for new position angles

$$\omega_1^+ = \omega_1 + \frac{\dot{\omega}_1 + \dot{\omega}_1^+}{2} \Delta t$$

$$\omega_2^+ = \omega_2 + \frac{\dot{\omega}_2 + \dot{\omega}_2^+}{2} \Delta t$$

$$\omega_3^+ = \omega_3 + \frac{\dot{\omega}_3 + \dot{\omega}_3^+}{2} \Delta t$$

so that a new transformation $[E^T C]^+$ may be found. In addition to the rotational degrees of freedom we have

$$\dot{\bar{R}}_{EC}^+ = \dot{\bar{R}}_{EC} + \frac{1}{m_C} \{F_x \ F_y \ F_z\} [C^T E]^T \Delta t \begin{Bmatrix} \bar{i} \\ \bar{j} \\ \bar{k} \end{Bmatrix} + \frac{T}{m_R} \Delta t \bar{i}_E$$

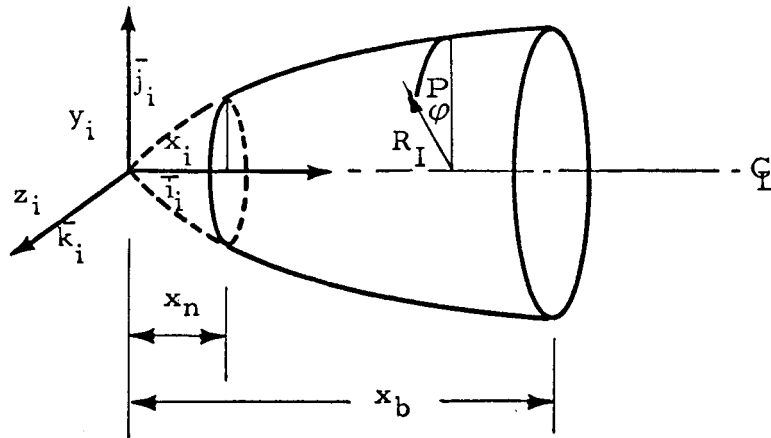
and

$$\bar{R}_{EC}^+ = \bar{R}_{EC} + \frac{\dot{\bar{R}}_{EC} + \dot{\bar{R}}_{EC}^+}{2} \Delta t$$

B.3 SURFACE GEOMETRY

A body is assumed to be a composite of simple shapes each with their own coordinate system. Since the body is not deformable, a transformation exists which is invariant with time which relates the subshape to the composite shape coordinate system. Three basic shapes are considered: (a) a conic shape, (b) a rectangular plate, and (c) a circular plate.

B.3.1 Conic Shape Coordinate System



A point P in the coordinate system is located at

$$\bar{P} = x_I \bar{i}_I + y_I \bar{j}_I + z_I \bar{k}_I$$

A point constrained to be on the surface, however, will satisfy the relation

$$S_I(x_I, y_I, z_I) = 0$$

but

$$R_I = \left\{ y_I^2 + z_I^2 \right\}^{1/2}$$

while in terms of the angle φ

$$y_I = R_I \cos \varphi$$

$$z_I = R_I \sin \varphi$$

Let the equation of the surface be

$$R_I - a \left\{ \sqrt{b + cx_I + dx_I^2} + e \right\} = 0 \quad x_n \leq x_I \leq x_b$$

With the above relations any point on the surface may easily be found as a function of x_I and φ . Since the end result is to be a pressure integration, then these variables are chosen as independent for the purposes of the integration.

The normal to the surface is

$$\bar{n} = \frac{\nabla S}{|\nabla S|} = \left(\frac{\partial S}{\partial x} \bar{i}_I + \frac{\partial S}{\partial y} \bar{j}_I + \frac{\partial S}{\partial z} \bar{k}_I \right) / |\nabla S|$$

which is just

$$\bar{n} = \left\{ -\frac{a}{2} \frac{(c+2 dx)}{R_I} \bar{i}_I + \frac{y_I}{R_I} \bar{j}_I + \frac{z_I}{R_I} \bar{k}_I \right\} / |\nabla S|$$

or

$$\bar{n} = \left\{ -\frac{a}{2} \frac{(c+2 dx)}{R_I} \bar{i}_I + \cos\varphi \bar{j}_I + \sin\varphi \bar{k}_I \right\} / |\nabla S|$$

where of course

$$|\nabla S| = \sqrt{\frac{a^2}{4 R_I^2} (c+2 dx)^2 + 1}$$

The origin of the conic shape is related to the structure origin by

$$\bar{R}_{CI} = x_{CI} \bar{i}_C + y_{CI} \bar{j}_C + z_{CI} \bar{k}_C = \left\{ x_{CI} \ y_{CI} \ z_{CI} \right\} \begin{pmatrix} \bar{i} \\ \bar{j} \\ \bar{k} \end{pmatrix}_C$$

while the vector \bar{i}_I is related by

$$\bar{i}_I = \cos\alpha_I \bar{i}_C + \cos\beta_I \bar{j}_C + \cos\gamma_I \bar{k}_C = \left\{ \cos\alpha_I \ \cos\beta_I \ \cos\gamma_I \right\} \begin{pmatrix} \bar{i} \\ \bar{j} \\ \bar{k} \end{pmatrix}_C$$

The transformation $[T_{IC}]$ must now be formed. Since the body is axisymmetric any choice of directions for \bar{j}_I and \bar{k}_I will suffice so long as a mutually perpendicular set is defined. A simple means of doing this is to define an intermediate vector by permuting the direction cosines

$$\bar{\xi} = \cos\gamma_I \bar{i}_C + \cos\alpha_I \bar{j}_C + \cos\beta_I \bar{k}_C$$

then let

$$\bar{j}_I = \frac{\bar{i}_I \times \bar{\xi}_I}{|\bar{i}_I \times \bar{\xi}_I|} ; \quad \bar{k}_I = \bar{i}_I \times \bar{j}_I$$

then finally

$$\begin{pmatrix} \bar{i} \\ \bar{j} \\ \bar{k} \end{pmatrix}_I = [T_{IC}] \begin{pmatrix} \bar{i} \\ \bar{j} \\ \bar{k} \end{pmatrix}_C$$

A point on the surface is then, in composite coordinates

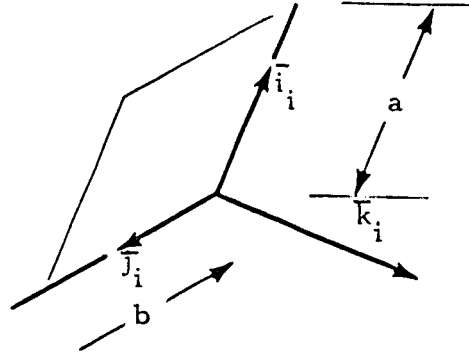
$$\begin{aligned} \bar{P} &= x_I \bar{i}_I + y_I \bar{j}_I + z_I \bar{k}_I + \bar{R}_{CI} \\ &= \left[\begin{pmatrix} x_I & y_I & z_I \end{pmatrix} [T_{IC}]^T + \begin{pmatrix} x_{CI} & y_{CI} & z_{CI} \end{pmatrix} \right] \begin{pmatrix} \bar{i} \\ \bar{j} \\ \bar{k} \end{pmatrix}_C \end{aligned}$$

And finally the composite system must be referred to the exit system so that a point on the surface will be

$$\bar{P} = \left(\begin{pmatrix} x_I & y_I & z_I \end{pmatrix} [T_{IC}]^T + \begin{pmatrix} x_{CI} & y_{CI} & z_{CI} \end{pmatrix} \right) [T_{CE}] \begin{pmatrix} \bar{i} \\ \bar{j} \\ \bar{k} \end{pmatrix}_E + \bar{R}_{EC}$$

B.3.2 Flat Plate Coordinate System

A flat rectangular plate is defined by two vectors



$$\bar{i}_I = \cos\alpha_I \bar{i}_C + \cos\beta_I \bar{j}_C + \cos\gamma_I \bar{k}_C$$

$$\bar{j}_I = \cos\alpha'_I \bar{i}_C + \cos\beta'_I \bar{j}_C + \cos\gamma'_I \bar{k}_C$$

and the lengths a and b . The normal to the surface is

$$\bar{n} = \pm \bar{k}_I = \pm \bar{i}_I \times \bar{j}_I$$

The transformation $[T_{CI}]$ is thus defined and

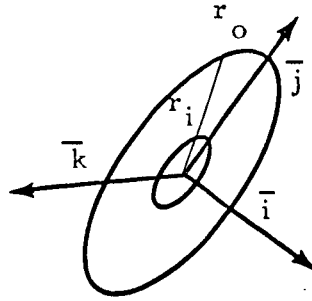
$$\begin{pmatrix} \bar{i} \\ \bar{j} \\ \bar{k} \end{pmatrix}_I = [T_{CI}] \begin{pmatrix} \bar{i} \\ \bar{j} \\ \bar{k} \end{pmatrix}_C$$

A point on the surface is then in composite coordinates

$$\bar{P} = + \{x_I \ y_I \ 0\} [T_{IC}]^T + \bar{R}_{CI}$$

B.3.3 Circular Flat Plate

A circular plate is defined by a vector through the center of the circle normal to the plane of the circle.



$$\bar{i} = \begin{Bmatrix} \cos\alpha \cos\beta \cos\gamma \\ \bar{i} \\ \bar{j} \\ \bar{k} \end{Bmatrix}_C$$

By permuting the direction cosines a new vector $\bar{\xi}$ is defined

$$\bar{\xi} = \begin{Bmatrix} \cos\gamma \cos\alpha \cos\beta \\ \bar{i} \\ \bar{j} \\ \bar{k} \end{Bmatrix}_C$$

$$\bar{j}_C = \frac{\bar{i} \times \bar{\xi}}{|\bar{i} \times \bar{\xi}|} \quad ; \quad \bar{k}_C = \bar{i} \times \bar{j}$$

B.4 RELATIVE VELOCITY

To perform a surface pressure calculation in any flow regime, local flow properties are required. These properties will be taken as those of the undisturbed stream at the point in question. The relative velocity of the flow

at the elemental area being evaluated is a function of flow velocity of the composite structure. We can see that

$$\bar{q}_{RC} = \left[\bar{q}_{FE} - \dot{\bar{R}}_{EC} \right] \left[T_{EC} \right].$$

Now the relative velocity at an elemental area is

$$\left[\bar{q}_{RI} = \bar{q}_{RC} \right] \left[T_{CI} \right].$$

The angle between the relative velocity vector and the surface of an elemental area is

$$\Theta = \pi/2 - \cos^{-1} \left\{ \frac{\bar{q}_{RI} \cdot \bar{n}}{\bar{q}_{RI}} \right\}.$$

The relative velocity and flow angle are now uniquely defined for each elemental area. This information is made available for a local pressure calculation using either continuum, free molecular or transitional flow theory.

APPENDIX C
FREE MOLECULAR AND TRANSITIONAL FORCES

FREE MOLECULAR AND TRANSITIONAL FORCES

C.1 FORCES PRODUCED IN FREE MOLECULAR FLOW

C.1.1 Introduction

Any body is said to experience specific "low density" effects when passing through a medium in which the mean free path of the molecules of the medium is large in comparison to the body dimensions. The magnitude of these "low density" effects is dependent upon such factors as shape, size and speed of the body, the surface condition of the body and surface monolayer composition of the body as well as the properties of the surrounding medium.

In defining flow regimes and flow types, a limiting type of flow, termed free molecular flow, is said to occur whenever the ratio of the molecular mean free path to the greatest projected body length perpendicular to the direction of molecular flow is 10 or greater. This ratio is commonly termed the Knudsen number and is the basic parameter used in defining the various flow regimes as:

| | |
|--------------------|------------------------|
| Free Molecule Flow | $Kn > 10$ |
| Transition Flow | $0.01 \leq Kn \leq 10$ |
| Continuum Flow | $Kn < 0.01$ |

Some experimental evidence seems to indicate that free molecule flow may occur at Knudsen numbers as low as 3 and sometimes does not occur until the Knudsen number is much greater than 10. However, the regime division shown above is quite sufficient for a general analysis and has been shown to be quite accurate in the majority of cases studied.

In the free-molecular and near free-molecular flight regimes, the dominant processes which control energy, momentum and mass transfer between the flow medium and a solid body are entirely different from those associated with continuum flight. In continuum flow, the transport properties are controlled by molecule-molecule collisions within the gas, while in free-molecule flow the transport properties depend entirely upon collisions of gas molecules with the body surface. These two flow regimes are separated by the transition regime, in which the change in dominant transport processes occurs in a gradual manner as the Knudsen number varies between 10 and .01. (See Appendix C.2).

A free molecule flow condition means simply that onrushing molecules, whose velocity vectors intercept a body, collide with that body uninfluenced by molecules which have already collided with the body and are rebounding. This can be understood when the large mean free paths associated with free-molecular flow are considered. Molecules collide only at distances so great that the oncoming molecular flux is not influenced by these molecular collisions. If environmental equilibrium can be assumed, a Maxwellian type flow exists and flow properties can be developed from gas dynamic theory and Maxwell's law of the distribution of molecular velocities. In this case it is also assumed that there are no shock waves formed and that the boundary layer is non-existent, thus assuring that the flow remains Maxwellian.

C.1.2 Effects of Molecule-Surface Interaction

Making the assumption that the incident and reflected molecules do not affect each other, the effect on the surface of the incident and reflected molecules can be computed separately. Thus the flow phenomena can be said to be governed by molecule-surface interactions.

To compute the forces on a body in a free molecule flow, the molecule-surface interaction must be specified. This specification requires assumptions in three areas:

1. The type of molecular reflection that occurs,
2. The momentum exchange between surface and molecule,
3. The energy exchange between surface and molecule.

There are two types of molecular reflection which may occur. They are: (1) specular in which the molecule hits the surface and is then reflected like a billiard ball, i.e., the angle of incidence equals the angle of reflection; and (2) diffuse in which the molecule hits the surface and is then re-emitted in a random direction. In both of these cases the velocity of the molecule which leaves the surface is dependent upon the amount of energy transfer between the surface and the molecule.

The degree of equilibrium attained between the molecule and the surface before the molecule is re-emitted, is measured by the energy accommodation coefficient, α , which is defined as

$$\alpha = \frac{E_i - E_r}{E_i - E_w}$$

where,

E_i is the total incident energy transported by the molecules to a unit area in unit time,

E_r is the total energy transported by the reflected molecules away from a unit surface area in unit time,

E_w is the total energy the reflected molecules would transport away from a unit surface area in unit time if they were re-emitted at the temperature of the surface, T_w .

If $E_r = E_i$, there is no energy exchange between the incident molecules and the surface and $\alpha = 0$. If the incident molecules and the surface reach thermal equilibrium before the molecules are re-emitted, $E_r = E_w$ and $\alpha = 1$. It is implicitly assumed in the definition of α that all the energies associated with those molecular degrees of freedom which enter into an energy exchange are accommodated to the same degree. In the equations which describe the forces acting on an element of area, T_r/T_i enters into the equation as a measure of this energy effect. Experimental values of the thermal accommodation coefficients obtained to date for surfaces and impinging molecules typical of those at orbital altitudes have the range $0.7 \leq \alpha \leq 1.0$.

The momentum transferred to the surface of a body in free-molecule flow is specified by momentum accommodation coefficients. Momentum

transport is normally expressed individually for the components tangent and normal to the surface. The tangential and normal momentum accommodation coefficients are defined as:

$$\sigma_t = \frac{\tau_i - \tau_r}{\tau_i - \tau_w}$$

$$\sigma_n = \frac{P_i - P_r}{P_i - P_w}$$

where,

τ_i and P_i are the incident tangential and normal momentum flux,

τ_r and P_r are the reflected tangential and normal momentum flux,

τ_w and P_w are the tangential and normal momentum flux for molecules emitted at the temperature of the surface.

In the case of diffusely emitted molecules, τ_w is equal to zero by definition, therefore σ_t may be written as

$$\sigma_t = \frac{\tau_i - \tau_r}{\tau_i}$$

For completely diffuse reflection, $\tau_r = \tau_w = 0$ and $\sigma_t = 1$ regardless of the degree of thermal accommodation. If any specular reflection occurs, the value of σ_t depends on the degree of thermal accommodation through τ_r . If there is complete specular reflection and no thermal accommodation, $\tau_r = \tau_i$ and $\sigma_t = 0$. If completely diffuse reflection and complete thermal accommodation occur, $\sigma_n = 1$, if completely specular reflection and no thermal accommodation occur, $\sigma_n = 0$. For any type of reflection between these two limits, σ_n depends on the degree of thermal accommodation that occurs. This is different from σ_t which is equal to one for completely diffuse reflection regardless of the degree of thermal accommodation which occurs. σ_t depends on the degree of thermal accommodation which occurs only when there is some specular reflection taking place.

Unfortunately, although the concept of a molecule-surface interaction goes back to Maxwell and Knudsen, there is a considerable lack of both theoretical and experimental information concerning the processes occurring at a gas-solid interface. For this reason, in the present analysis a diffuse type reflection ($\sigma_t = \sigma_n = 1$) is assumed. It will also be assumed that $E_r = E_w$ or $T_r = T_w$ which means that there is complete energy accommodation. Available experimental evidence seems to indicate that for the type of surfaces used in most spacecraft, the assumption of completely diffuse reflection is legitimate. Complete energy accommodation may or may not be a good assumption; however, lack of known data make this assumption a necessity. The effect of variable accommodation coefficients on the various aerodynamic coefficients are shown in graphical form in Reference C-5. If more data should become available, the equations can be modified to facilitate using σ 's and α 's of any required value. Equations have also been derived for the force coefficients, when specular reflection is assumed.

C.1.3 The Force on an Element of Area in a Free Molecule Flow

Making several assumptions as to the nature of the flow around a body, a straightforward (though tedious) calculation of the forces on that body in free molecule flow may be made. Because of the length of this derivation, a step-by-step presentation will not be made here but rather a summary of the assumptions will be made, as well as a brief description of the method of solution and the final results. If a detailed derivation is required, reference is made to Reference C-1 by Sentman and a less detailed description in Reference C-2 by Patterson.

The following assumptions were made in the force equation derivation:

- Molecular velocity distribution which is ahead of the body is Maxwellian,
- There is diffuse reflection of the molecules from the body,
- Surfaces are non-concave. (If we do not make this assumption, we must take into account the forces due to the molecules that have been reflected from other parts of the body.)

If the above assumptions are made and, of course, if the free molecular assumption that the molecules do not collide with each other is made, the total force on an element of area can be computed. This computation is made by computing the forces produced by the incident and reflected molecules, using the kinetic theory of gases and then adding them. The resulting equation is:

$$\frac{dF}{dA} = \frac{\zeta}{2\beta} \left\{ \frac{1}{\sqrt{\pi}} (k\epsilon + l\gamma + t\eta) \left[\gamma S^2 \sqrt{\pi} (1 + \operatorname{erf} \gamma S) + S e^{-\gamma^2 S^2} \right] + \frac{l}{2} (1 + \operatorname{erf} \gamma S) + \frac{l}{2} \sqrt{\frac{T_r}{T_i}} \left[\gamma S \sqrt{\pi} (1 + \operatorname{erf} \gamma S) + e^{-\gamma^2 S^2} \right] \right\}$$

where

- ζ = density of the molecules
- β = $1/2 R T_i$ (dimensions of sec^2/ft^2)
- R = gas constant
- T_i = incident molecular temperature
- T_r = reflected molecular temperature and is equal to the body temperature for complete energy accommodation
- S = molecular speed ratio
= mass velocity/most probable molecular velocity
= $V/\sqrt{2 R T_i}$
- k, l, t = direction cosines between the local x, y, and z axes and the desired force direction (x, y, and z represent a natural coordinate system with y normal to the surface)
- ϵ, γ, η = direction cosines between the local x, y, and z axes and the mass velocity vector
- $\operatorname{erf} \gamma S$ = the error function of γS

This equation is exact within the physical assumptions of kinetic theory, free molecule flow, diffuse molecular reemission, and non-concave surfaces. It must now be integrated over the entire body to give the total force.

C.2 TRANSITION FLOW AERODYNAMIC CHARACTERISTICS

C.2.1 Introduction

In some cases involving the flow of a gas over a body, the body may be within a region of flow known as the transition regime, defined in terms of the Knudsen number as, $0.01 \leq Kn \leq 10$ (see Appendix C.1). Molecules rebounding from the vehicle in this regime experience collisions which occur closer and closer to the vehicle. Eventually, some of these molecular collisions occur close enough to the vehicle that some incoming molecules, which would otherwise strike the vehicle, are knocked out of the way. The incident stream of molecules is thus attenuated, and there is a reduction of energy and momentum transfer to the vehicle relative to the freestream energy and momentum flux. This flow regime is frequently subdivided into various sub-regions: first collision, transitional, fully merged, incipient merged, viscous layer, and vorticity interaction regions. Through these sub-regions, aerodynamic force coefficients are a function of Knudsen number as well as Mach number.

C.2.2 Definition of Aerodynamic Coefficients in Transition Flow

Attempts to extend continuum and free molecule theories into the transition regime have been made, resulting in the development of several approximate theories, all of which have limited ranges of applicability. It is apparent from all available experimental data, however, that the transition aerodynamic force coefficients lie within a region bounded on the low end by continuum values and on the high end by free molecule values.

As an approach to the problem of estimating transition force coefficients, LMSC/HREC developed an empirical equation applicable to the determination of these parameters. Experimental transition force data on spheres, cylinders and reentry vehicles from several references were analyzed, resulting in a sine-squared variation with the logarithm of the Knudsen number for the force coefficients. This variation was then used to develop the following empirical curve-fit relationship,

$$A C_{\text{tran}} = A C_{\text{cont}} + (A C_{\text{fm}} - A C_{\text{cont}}) \sin^2 \left[\left(\pi \right) \left(\frac{1}{3} + \frac{1}{6} \log_{10} \text{Kn} \right) \right]$$

where:

| | |
|---------------------|--|
| $A C_{\text{tran}}$ | is any aerodynamic coefficient in transition flow |
| $A C_{\text{fm}}$ | is any aerodynamic coefficient (corresponding to $A C_{\text{tran}}$) in free-molecular flow |
| $A C_{\text{cont}}$ | is any aerodynamic coefficient (corresponding to $A C_{\text{tran}} + A C_{\text{fm}}$) in continuum flow |
| Kn | is the Knudsen number $0.01 \leq \text{Kn} \leq 10.0$. |

The equation yields a smooth transition from free molecule to continuum flow, as shown in Figure C-1 and is considered to be the best method presently available for estimating aerodynamic force coefficients over the entire transition regime.

APPENDIX C REFERENCES

- C-1 Sentman, Lee H., "Free Molecule Flow Theory and Its Application to the Determination of Aerodynamic Forces," Lockheed Missiles & Space Company, Sunnyvale, California, LMSC-448514, 1 October 1961.
- C-2 Patterson, G. N., Molecular Flow of Gases, John Wiley & Sons, Inc., New York, 1956.
- C-3 Shirley, B. H., "Free Molecule Aerodynamic Coefficients," Paper presented at "Southeastern Symposium in Missiles and Aerospace Vehicles Sciences," American Astronautical Society, Huntsville, Alabama December 1966.
- C-4 Shirley, B. H., and W. H. Sims, "Study of Drag Coefficients for Unusual Vehicle Configurations," February Progress Report, LMSC/HREC A782420, March 1966.
- C-5 Shirley, B. H., "Methods Used in Determining Free Molecule Aerodynamic Force Coefficients," LMSC/HREC A782143, January 1966.

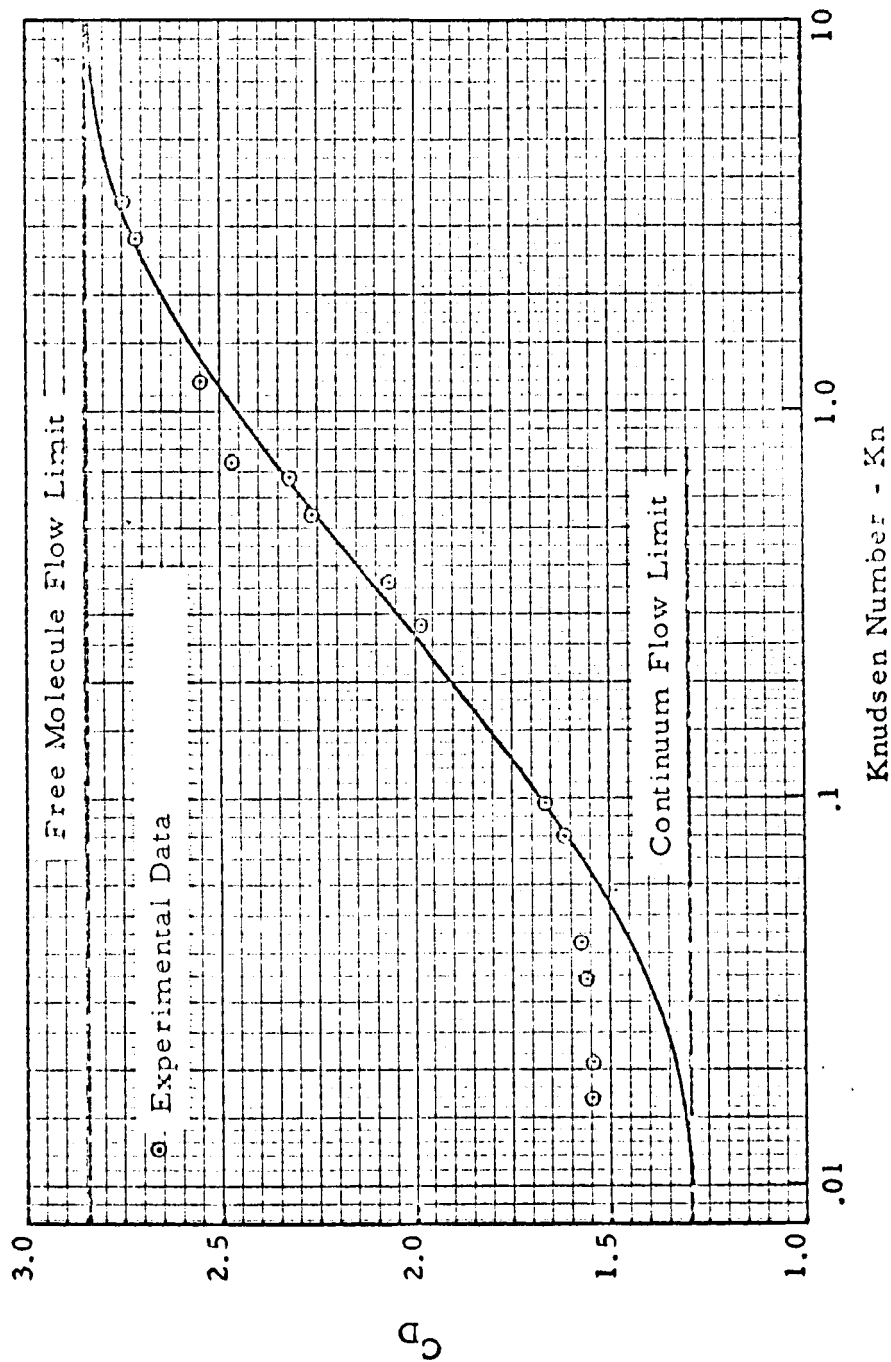


Figure C-1 - LMSC/HREC Transition Force Coefficients Empirical Relationship (Cylinder at $M=6$)

APPENDIX D
FREE MOLECULAR HEATING

APPENDIX D NOMENCLATURE

| | |
|-----------|---|
| \vec{C} | molecular velocity (ft/sec) |
| E | rate at which total energy strikes a surface (Btu/ft ² -sec) |
| e_{ij} | rate at which a specific type of energy strikes a surface (Btu/ft ² -sec) |
| erf(x) | error function of x |
| f | Maxwell-Boltzmann distribution function |
| g | gravitational constant = $32.2 \frac{\text{ft-lbf}}{\text{lbm-sec}^2}$ |
| h | static enthalpy (Btu/lbm) |
| J | mechanical equivalent of heat = $778 \frac{\text{ft-lbf}}{\text{Btu}}$ |
| j | number of degrees of freedom |
| k | Boltzmann's constant = $5.66 \times 10^{-24} \frac{\text{ft-lbf}}{\text{molecule}^\circ\text{R}}$ |
| m | mass of a molecule (lbm) |
| N | rate at which molecules strike a unit surface per unit time $\left(\frac{\text{molecules}}{\text{ft}^2\text{-sec}} \right)$ |
| n | number density $\left(\frac{\text{molecules}}{\text{ft}^3} \right)$ |
| p | static pressure (lbf/ft ²) |
| q | heat transfer rate (Btu/ft ² -sec) |
| R | gas constant $\left(\frac{\text{ft-lbf}}{\text{lbm}^\circ\text{R}} \right)$ |

NOMENCLATURE (Continued)

| | |
|------------------|--|
| S | molecular speed ratio |
| T | temperature ($^{\circ}\text{R}$) |
| \vec{U} | freestream velocity (ft/sec) |
| U_{TOT} | total internal energy (Btu/lbm) |
| u | internal energy (Btu/molecule) |
| α | accommodation coefficient |
| γ | ratio of specific heats |
| θ | angle between freestream direction and positive y direction of plate |
| ρ | density (lbm/ft ³) |

Subscripts

| | |
|----------|--|
| $(\)_b$ | pertaining to back-side conditions |
| $(\)_i$ | property evaluated at freestream temperature |
| $(\)_i$ | due to internal energy |
| $(\)_k$ | due to kinetic energy |
| $(\)_w$ | property evaluated at temperature of wall |

FREE MOLECULAR HEATING

D.1 GENERAL DISCUSSION

In the free molecular flow regime, the aerodynamic heating rate to an element of surface area can be calculated from an energy balance.

$$q = E_i - E_r \quad (D.1)$$

where

- q = heat transfer rate
- E_i = rate at which total energy is incident on the surface area
- E_r = rate at which total energy is reflected from the surface area

Because of the assumption in free molecular flow that the molecules have a Maxwellian velocity distribution, there is a temperature associated with each of the energy rates, E_i and E_r . Although the temperature of the incoming or incident molecules is usually a well-defined quantity, the temperature of the reflected molecules is a function of the particular gas-surface interaction and is not known. It is common practice in all free molecular theory to combine this uncertainty into a parameter called the accommodation coefficient, α , defined by

$$\alpha = \frac{E_i - E_r}{E_i - E_w}$$

where

- E_w = rate at which total energy is reflected from the surface area assuming that the velocity distribution of the reflected molecules is characterized by the wall or surface temperature, T_w .

Note the type of gas-surface interaction under consideration here. It is hypothesized that the incoming molecules can be described with a Maxwellian velocity distribution characterized by a temperature, T_i . All of the molecules striking the surface are "captured" by the surface and give up all their energy to the surface. At some later time (the length of time is not important to this analysis), the molecules are diffusely emitted or "reflected" from the surface as if they originated from an infinite reservoir with zero mean velocity. Again, their velocity distribution is considered to be Maxwellian, characterized by a temperature T_r . This gas-surface interaction must conserve mass. The parameter α is considered to be a measure of how well the surface accommodates the incident energy. Thus, Equation (D.1) can be written

$$q = \alpha(E_i - E_w) \quad (D.2)$$

The maximum heat transfer occurs when α has a value of unity.

The total energy associated with each one of the molecules striking the surface consists of kinetic energy and internal energy. It is convenient to define

$$E_i = e_{ik} + e_{ii} \quad (D.3)$$

where

$$\begin{aligned} e_{ik} &= \text{rate at which kinetic energy is transferred to the surface} \\ &\quad \text{by the incident molecules assuming their velocity distribution} \\ &\quad \text{is characterized by the temperature } T_i \\ e_{ii} &= \text{rate at which internal energy is transferred to the surface} \\ &\quad \text{by the incident molecules assuming their velocity distribution} \\ &\quad \text{is characterized by the temperature } T_i \end{aligned}$$

Similarly, the total energy carried away from the surface by the reflected or emitted molecules can be written as

$$E_w = e_{wk} + e_{wi} \quad (D.4)$$

where

e_{wk} = rate at which kinetic energy is carried away from the surface by the emitted molecules, assuming that the velocity distribution of the emitted molecules is characterized by the temperature, T_w

e_{wi} = rate at which internal energy is carried away from the surface by the emitted molecules, assuming that the velocity distribution of the emitted molecules is characterized by the temperature, T_w

T_w = temperature of the wall

Thus, Equation (D.2) can be written

$$q = \alpha [(e_{ik} - e_{wk}) + (e_{ii} - e_{wi})] \quad (D.5)$$

It is desired to calculate the heat transfer to a flat plate of unit area at an angle of attack, θ , to the incoming flow.

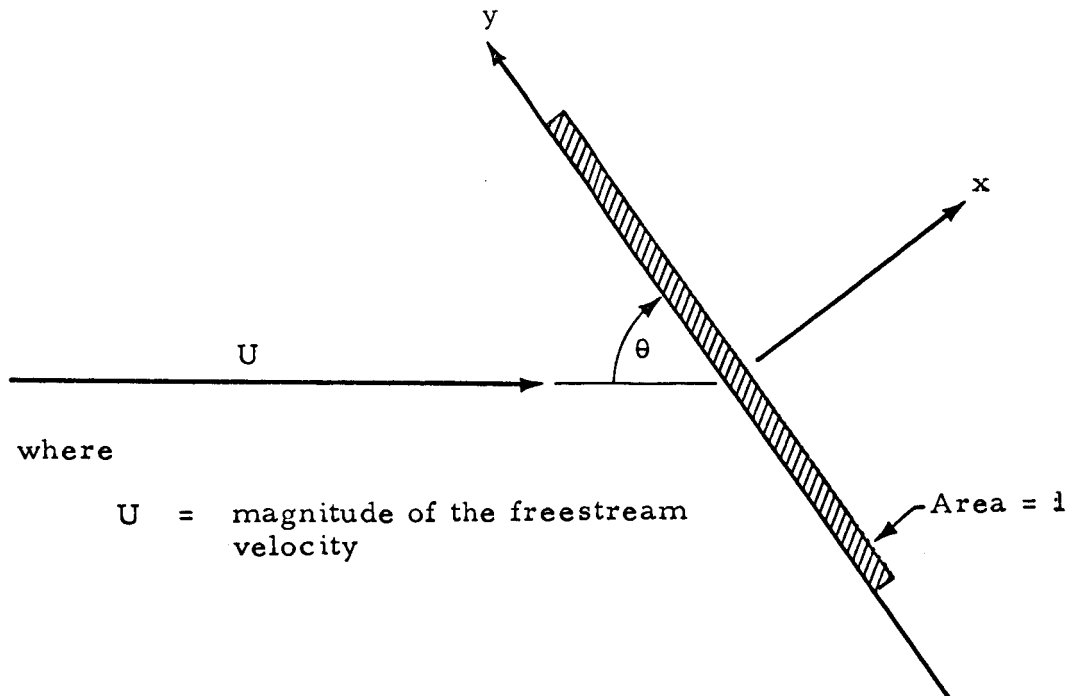


Figure D-1

By definition, the front side of the plate is the negative x side and the back side is the positive x side. Both sides of the plate experience heating.

D.2 FRONT SIDE HEATING

To find an expression for the front side heating, all the terms in Equation (D.5) must be evaluated. If \vec{C} is the velocity vector of a molecule, and m_i is the mass of one molecule, then the molecule possesses $\frac{1}{2} m_i |\vec{C}|^2$ kinetic energy. Total kinetic energy transferred to any point is found by integrating the product of f and $\frac{1}{2} m_i |\vec{C}|^2$ over the appropriate region of velocity space. Thus, for the quantity e_{ik} ,

$$e_{ik} = \iiint \frac{1}{2} m_i (C_x^2 + C_y^2 + C_z^2) f dV \quad (D.6)$$

where

C_x, C_y, C_z = Cartesian components of the molecular velocity \vec{C}

f = Maxwell-Boltzmann distribution function

$$= n_i \left(\frac{m_i}{2\pi k T_i} \right)^{3/2} e^{-\frac{m_i}{2kT_i} [(C_x - U_x)^2 + (C_y - U_y)^2 + (C_z - U_z)^2]}$$

n_i = number density of incident flow

T_i = temperature of the incident flow

U_x, U_y, U_z = components of freestream velocity vector

dV = differential element of velocity flux space

Since only those molecules striking the front surface will transfer energy to the front surface, the integration over velocity space must include only those molecules having velocity components in the positive C_x direction. Thus, the differential element of velocity flux space will be

$$dV = C_x dC_x dC_y dC_z$$

and the integral for e_{ik} becomes

$$e_{ik} = \int_{-\infty}^{+\infty} \int_0^{+\infty} \frac{m_i n_i}{2} \left(\frac{m_i}{2\pi k T_i} \right)^{3/2} (C_x^2 + C_y^2 + C_z^2) e^{-\frac{m_i}{2kT_i} [(C_x - U_x)^2 + (C_y - U_y)^2 + (C_z - U_z)^2]} C_x dC_x dC_y dC_z$$

From Figure D-1, it is clear that the components of the freestream velocity are

$$U_x = U \sin \theta$$

$$U_y = -U \cos \theta$$

$$U_z = 0$$

Completing the integration in Equation (D.7),

$$e_{ik} = \frac{\rho_i R_i T_i}{J} \left(\frac{R_i T_i g}{2\pi} \right)^{1/2} \left\{ (2 + S^2) e^{-S^2 \sin^2 \theta} + \pi^{1/2} S \sin \theta (1 + \operatorname{erf} S \sin \theta) \left(\frac{5}{2} + S^2 \right) \right\} \quad (D.8)$$

where

$$\rho_i = m_i n_i = \text{density of the incident flow}$$

$$R_i = k/m_i = \text{gas constant of the incident flow}$$

S = molecular speed ratio

$$= \frac{U}{\sqrt{2R_i g T_i}}$$

To find an expression for e_{wk} , the boundary conditions of the gas-surface interaction process must be imposed on the system. First, the number of molecules which reach the front side of the unit area per unit time must be computed. From the geometry of Figure D-1 and consideration of kinetic theory,

$$N_i = \iiint f dV$$

$$N_i = n_i \left(\frac{m_i}{2\pi k T_i} \right)^{3/2} \iiint_{-\infty}^{+\infty} e^{-\frac{m_i}{2k T_i} [(C_x - U_x)^2 + (C_y - U_y)^2 + (C_z - U_z)^2]} C_x dC_x dC_y dC_z$$

Completing the integration,

$$N_i = n_i \left(\frac{R_i T_i g}{2\pi} \right)^{1/2} \left[e^{-S^2 \sin^2 \theta} + \pi^{1/2} S \sin \theta (1 + \operatorname{erf} S \sin \theta) \right] \quad (D.9)$$

The quantity N_i represents the number of incident molecules striking the unit surface in a unit time. These molecules are "captured" by the surface and later emitted or reflected from the surface as if they came from an infinite reservoir held at temperature T_w with zero mean velocity. However, the number of molecules reflected from the surface per unit time, N_r , must be equal to the number of molecules striking the surface per unit time evaluated at "reservoir conditions." Thus

$$N_r = N_i \left| \begin{array}{l} n = n_w \\ T = T_w \\ R = R_w \\ U = 0 \end{array} \right.$$

Applying this condition to Equation (D.9),

$$N_r = n_w \left(\frac{R_w T_w g}{2\pi} \right)^{1/2} \quad (D.10)$$

But since at the surface, $N_i = N_r$ at all times, then from Equations (D.9) and (D.10),

$$n_w = n_i \left(\frac{R_i T_i}{R_w T_w} \right)^{1/2} \left[e^{-S^2 \sin^2 \theta} + \pi^{1/2} S \sin \theta (1 + \operatorname{erf} S \sin \theta) \right] \quad (D.11)$$

Equation (D.11) gives the necessary expression for the number density of the reflected molecules in terms of the number density of the incident molecules and the temperature of the wall.

The amount of kinetic energy stored in the reservoir, which is emitted from the surface, can be found by imposing the boundary conditions on the incident kinetic energy, viz.,

$$e_{wk} = e_{ik} \left| \begin{array}{l} n = n_w \\ T = T_w \\ R = R_w \\ U = 0 \end{array} \right.$$

Thus, from Equation (D.8)

$$e_{wk} = \frac{2 n_w k T_w}{J} \left(\frac{R_w T_w g}{2\pi} \right)^{1/2}$$

Substituting the expression from Equation (D.11) for n_w ,

$$e_{wk} = \frac{2 \rho_i R_i T_w}{J} \left(\frac{R_i T_i}{2\pi} \right)^{1/2} \left\{ e^{-S^2 \sin^2 \theta} + \pi^{1/2} S \sin \theta \cdot (1 + \operatorname{erf} S \sin \theta) \right\} \quad (D.12)$$

In addition to the heating caused by transfer of kinetic energy, the surface also experiences heating due to the transfer of internal energy by the incident molecules. Because of the way in which the energy balance at the surface is formulated, the amount of internal energy which contributes to the heating is the total internal energy minus that part of the internal energy due to translational degrees of freedom - which has already been accounted for. In the conventional free molecular heating theory for cold air (Reference D-1), the molecules under consideration are, at most, diatomic. Thus, there exists a simple relationship between γ and the number of degrees of freedom, i.e.,

$$\gamma = 1 + \frac{2}{j} \quad (D.13)$$

where

γ = ratio of specific heats

j = number of degrees of freedom

Using the principle of equipartition of energy and the above relationship, the amount of internal energy due to $j - 3$ degrees of freedom can be readily calculated. Now, if the problem is changed such that the incident flow may be composed of high temperature gases from a rocket engine exhaust, then this theory is no longer adequate.

In the search for a new solution, a digression into kinetic theory will be helpful. It is well known that the total internal energy stored by N molecules of a gas in thermodynamic equilibrium at a temperature T is given by

$$U_{TOT} = NkT^2 \left(\frac{\partial \ln f}{\partial T} \right)_v \quad (D.14)$$

where

f = total partition function

Depending upon the complexity of the molecules and the level of excitation, f could be an extremely complicated function. However, it will always be given in the form,

$$f = (f_{trans})(f_{rot})(f_{vib})(\dots)(\dots) \quad (D.15)$$

where

f_{trans} = translational partition function

f_{rot} = rotational partition function

f_{vib} = vibrational partition function

and so on.

Hence, if we know f for any complex molecule, we can find an expression for the total internal energy of the N molecules using Expression (D.1).

$$U_{TOT} = NkT^2 \frac{\partial}{\partial T} \left\{ \ln f_{trans} + \ln f_{rot} + \ln f_{vib} + \dots + \dots \right\} \Big|_v \quad (D.16)$$

From this expression, it is clear that the total internal energy is composed of contributions from each "type" of freedom in the complex molecule.

$$U_{TOT} = U|_{\text{due to translation}} + U|_{\text{due to rotation}} + U|_{\text{due to vibration}} + \dots$$

As has been mentioned, the quantity of interest is the total internal energy minus the contribution of the translational degrees of freedom. Thus,

$$U_S = U_{TOT} - NkT^2 \frac{\partial}{\partial T} (\ln f_{trans})_v \quad (D.17)$$

is a direct method to calculate this quantity. If the velocity of a molecule is given by

$$\vec{C} = C_x \vec{i} + C_y \vec{j} + C_z \vec{k}$$

then the translational partition function is

$$f_{trans} = \exp \left[-\frac{m}{2kT} (C_x^2 + C_y^2 + C_z^2) \right] \quad (D.18)$$

Substituting Equation (D.18) into Equation (D. 17)

$$U_S = U_{TOT} - N \left(\frac{mC^2}{2} \right)$$

where

$$C^2 = C_x^2 + C_y^2 + C_z^2$$

or on the basis of one molecule,

$$u_S = u_{TOT} - \frac{mC^2}{2} \quad (D.19)$$

Although the total internal energy of a complicated molecule of gas, U_{TOT} , is usually very difficult to describe by use of partition functions, it can be determined from thermodynamic relations if the assumption is made that the gas is in equilibrium at a temperature T , i.e.,

$$h = \text{total internal energy} + p/\rho J$$

where

h = static enthalpy per unit mass

p = static pressure

ρ = density

In terms of internal energy per molecule

$$u_{TOT} = \left(h - \frac{p}{\rho J} \right) \frac{\rho}{n} \left(\frac{\text{energy}}{\text{molecule}} \right) \quad (D.20)$$

Since it was assumed that h , p , ρ are thermodynamic properties of the gas at equilibrium, they are steady state values. Thus, it would seem reasonable to use the average or "steady state" value of C^2 in Equation (D.19). This average value is called a most probable value defined by

$$\overline{C^2} = \iiint_{-\infty}^{+\infty} C^2 f \, dV$$

$$\overline{C^2} = \frac{3kT}{m} \quad (D.21)$$

Thus, Equation (D.19) becomes

$$u_S = u_{TOT} - \frac{3}{2} kT \quad (D.22)$$

$$u_S = \left(h - \frac{p}{\rho J} \right) \frac{\rho}{n} - \frac{3}{2} kT \quad (D.23)$$

Since the thermodynamic equation of state relates the equilibrium properties of the gas, Equation (D.23) can be re-written as

$$u_S = \left(h - \frac{RT}{2J} \right) \frac{\rho}{n} \left(\frac{\text{energy}}{\text{molecule}} \right) \quad (\text{D.24})$$

where again, $R = k/m$

By using the method-of-characteristics plume which gives an accurate description of the local properties of the gas at every point in the flow field, the quantity u_S can easily be determined. Assuming that this accurate description of the properties exists, then no approximate relationship between γ and the number of degrees of freedom in the molecule is needed.

Now, the amount of internal energy incident on the surface can be calculated by multiplying the number of molecules incident on the surface per unit time, N_i , by the internal energy contribution of one molecule, u_S , i.e.,

$$e_{ii} = (N_i)(u_S)$$

Using Equation (D.9),

$$e_{ii} = \rho_i \left(\frac{R_i T_i g}{2\pi} \right)^{1/2} \left[h_i - \frac{R_i T_i}{2J} \right] \left\{ e^{-S^2 \sin^2 \theta} + \pi^{1/2} S \sin \theta (1 + \text{erf } S \sin \theta) \right\} \quad (\text{D.25})$$

Using a similar analysis for the reflected molecules, the internal energy is given by

$$u_{Sw} = \left(h_w - \frac{R_w T_w}{2J} \right) \frac{\rho_w}{n_w}$$

= reflected internal energy/molecule

and the amount of internal energy carried away from the surface by the reflected molecules is

$$e_{wi} = (N_r)(u_{Sw})$$

$$e_{wi} = \rho_i \left(\frac{R_i}{R_w} \right) \left(\frac{R_i T_i g}{2} \right)^{1/2} \left[h_w - \frac{R_w T_w}{2J} \right] \left\{ e^{-S^2 \sin^2 \theta} + \pi^{1/2} S \sin \theta (1 + \operatorname{erf} S \sin \theta) \right\} \quad (D.26)$$

The heat transfer rate to the front side of the unit surface is found by substitution of Equations (D.8), (D. 12), (D. 25) and (D. 26) into Equation (D.5). Thus,

$$\begin{aligned} \frac{qf}{\alpha} = & \frac{\rho_i R_i T_i}{J} \left(\frac{R_i T_i g}{2\pi} \right)^{1/2} \left\{ e^{-S^2 \sin^2 \theta} \left[2 \left(1 - \frac{T_w}{T_i} \right) + S^2 \right] \right. \\ & + \pi^{1/2} S \sin \theta (1 + \operatorname{erf} S \sin \theta) \left[S^2 + \frac{5}{2} - 2 \left(\frac{T_w}{T_i} \right) \right] \left. \right\} \\ & + \rho_i \left(\frac{R_i T_i g}{2\pi} \right)^{1/2} \left\{ \left[h_i - \frac{R_i T_i}{2J} \right] - \frac{R_i}{R_w} \left[h_w - \frac{R_w T_w}{2J} \right] \right\} \\ & \left[e^{-S^2 \sin^2 \theta} + \pi^{1/2} S \sin \theta (1 + \operatorname{erf} S \sin \theta) \right] \end{aligned} \quad (D.27)$$

D.3 BACK SIDE HEATING

The heat transfer to the back side of the flat plate shown in Figure D-1 is also found from an energy balance at the surface.

$$\frac{q_b}{\alpha} = (e_{ikb} - e_{wkb}) + (e_{iib} - e_{wib}) \quad (D.28)$$

where

e_{ikb} = rate at which kinetic energy is transferred to the backside surface by the incident molecules, assuming that their velocity distribution is characterized by the temperature, T_i

e_{wkb} = rate at which kinetic energy is carried away from the backside surface by the reflected molecules, assuming that their velocity distribution is characterized by the temperature, T_w .

e_{iib} = rate at which internal energy is transferred to the backside surface by the incident molecules, assuming that their velocity distribution is characterized by the temperature, T_w .

e_{wib} = rate at which internal energy is carried away from the backside surface by the reflected molecules, assuming that their velocity distribution is characterized by the temperature, T_w .

The rate at which kinetic energy is transferred to the backside of the surface is found in a similar manner to that for the front side, i.e.,

$$e_{ikb} = \iiint \frac{1}{2} m_i (C_x^2 + C_y^2 + C_z^2) f dV$$

Since only those molecules striking the backside surface will transfer energy to the surface, the integration over velocity space must include only those molecules having velocity components in the negative C_x direction. For this region of velocity space, the differential velocity flux element becomes

$$dV = -C_x dC_x dC_y dC_z$$

and

$$\begin{aligned}
e_{ikb} = & \iiint_{-\infty}^{+\infty} \frac{m_i n_i}{2} \left(\frac{m_i}{2\pi k T_i} \right)^{3/2} (C_x^2 + C_y^2 + C_z^2) \\
& e^{-\frac{m_i}{2kT_i} [(C_x - U_x)^2 + (C_y - U_y)^2 + (C_z - U_z)^2]} \\
& (-C_x) dC_x dC_y dC_z
\end{aligned} \tag{D.29}$$

Again, the velocity components of the freestream flow are

$$\begin{aligned}
U_x &= U \sin \theta \\
U_y &= -U \cos \theta \\
U_z &= 0
\end{aligned}$$

Completing the integration,

$$\begin{aligned}
e_{ikb} = & \frac{\rho_i R_i T_i}{J} \left(\frac{R_i T_i g}{2\pi} \right)^{1/2} \left\{ e^{-S^2 \sin^2 \theta} (2 + S^2) \right. \\
& \left. - \pi^{1/2} S \sin \theta \left(\frac{5}{2} + S^2 \right) (1 - \operatorname{erf} S \sin \theta) \right\}
\end{aligned} \tag{D.30}$$

The three other terms in Equation (D.28) are generated in the same manner as they were in the front side heating calculations. The only difference being the different region of velocity space which governs the limits of the integration. The results of the computations are

$$\begin{aligned}
e_{wkb} = & 2 \frac{\rho_i R_i T_w}{J} \left(\frac{R_i T_i g}{2} \right)^{1/2} \left[e^{-S^2 \sin^2 \theta} \right. \\
& \left. - \pi^{1/2} S \sin \theta (1 - \operatorname{erf} S \sin \theta) \right]
\end{aligned} \tag{D.31}$$

$$e_{iib} = \rho_i \left(\frac{R_i T_i g}{2} \right)^{1/2} \left[h_i - \frac{R_i T_i}{2J} \right] \left\{ e^{-S^2 \sin^2 \theta} - \pi^{1/2} S \sin \theta (1 - \operatorname{erf} S \sin \theta) \right\} \quad (D.32)$$

$$e_{wib} = \rho_i \left(\frac{R_i}{R_w} \right) \left(\frac{R_i T_i g}{2\pi} \right)^{1/2} \left[h_w - \frac{R_w T_w}{2J} \right] \left\{ e^{-S^2 \sin^2 \theta} - \pi^{1/2} S \sin \theta (1 - \operatorname{erf} S \sin \theta) \right\} \quad (D.33)$$

Thus, the heat transfer rate to the backside surface is given by Equation (D.28)

$$\begin{aligned} \frac{q_b}{\alpha} = & \frac{\rho_i R_i T_i}{J} \left(\frac{R_i T_i g}{2\pi} \right)^{1/2} \left\{ e^{-S^2 \sin^2 \theta} \left[S^2 + 2 \left(1 - \frac{T_w}{T_i} \right) \right] \right. \\ & - \pi^{1/2} S \sin \theta (1 - \operatorname{erf} S \sin \theta) \left(S^2 + \frac{5}{2} - 2 \frac{T_w}{T_i} \right) \Big\} \\ & + \rho_i \left(\frac{R_i T_i g}{2\pi} \right)^{1/2} \left\{ \left[h_i - \frac{R_i T_i}{2J} \right] - \frac{R_i}{R_w} \left[h_w - \frac{R_w T_w}{2J} \right] \right\} \\ & \left[e^{-S^2 \sin^2 \theta} - \pi^{1/2} S \sin \theta (1 - \operatorname{erf} S \sin \theta) \right] \end{aligned} \quad (D.34)$$

In determining the heating rate to a large body or vehicle, the surface area is visualized as a great number of differential areas which are considered to be flat plates at an angle of attack to the freestream flow. Equations (D.27) and (D.33) are used to calculate the heating rates, depending on whether the element of surface area is exposed to the freestream velocity (front side) or not (backside). This is possible because the mechanism for energy transfer

to an element of surface area is not influenced by any preceding or adjacent phenomena.

The theory of free molecular heat transfer presented here is an extension of the existing theory in that it includes an accurate method of determining heat transfer to surfaces exposed to gases with arbitrary composition and temperature. This is necessary for any problems where the gas surrounding the vehicle is not composed of diatomic molecules at low temperatures. However, the accuracy of the new method depends on how accurately the local thermodynamic properties of the gas can be determined.

APPENDIX D
REFERENCES

- D-1 Oppenheim, A. K., "Generalized Theory of Convective Heat Transfer in a Free-Molecule Flow," J. Aeron. Sci., January 1963, p. 49.

APPENDIX E
CONVECTIVE HEATING

APPENDIX E NOMENCLATURE

| | |
|------------|--|
| C_p | specific heat (Btu/slug) |
| H | enthalpy (Btu/slug) |
| K | thermal conductivity (Btu/ft ² -sec ^{°R}) |
| Nu | Nusselt number |
| Pr | Prandtl number ($\mu C_p / K$) |
| q | heating rate (Btu/ft ² -sec) |
| r | radial coordinate (feet) |
| Re | Reynolds number ($V \rho / \mu$) |
| S | surface length (feet) |
| T | temperature (^{°R}) |
| V | velocity (feet/second) |
| x | axisymmetric centerline coordinate (feet) |
| δ | flow to body deflection angle ~ degrees |
| θ_c | cone half angle ~ degrees |
| μ | viscosity (slugs-ft/sec) |
| ρ | density (slugs/ft ³) |

Subscripts

| | |
|------|--|
| aw | adiabatic wall |
| f | final conditions |
| i | initial conditions |
| L | flow conditions at boundary layer edge |

NOMENCLATURE (Continued)

Subscripts (Cont'd)

| | |
|-----|---|
| sf | final transformed characteristic length |
| sfo | final transformed characteristic length off windward streamline |
| si | initial transformed characteristic length |
| sp | stagnation point |
| w | flow conditions at body wall temperature |
| * | flow conditions at reference temperature |

CONVECTIVE HEATING

E.1 METHOD OF APPROACH

To facilitate rapid and accurate estimates of the heating rates to a body immersed in a rocket exhaust plume, the heating rate distributions over each body shape are calculated as if the body were immersed in a uniform gas environment. The local heating rate to each body segment is expressed as a ratio to that which would be experienced at the stagnation point on a one-foot radius hemisphere. A real gas solution for the stagnation point heating rate is calculated for each time step and subsequently used to obtain a local heating rate from the heating rate ratio obtained by methods similar for those used for non-reacting air. For the enthalpies obtainable in most exhaust plumes, Sutherland's Viscosity Law and the similar conductivity relationship have been found to be valid to the order in magnitude necessary for obtaining these heating ratios. In calculating the final heating rate the programmer may (1) specify real gas viscosities, conductivities, and specific heat, or (2) use approximate formulae in the program to evaluate the transport properties.

An analytic most-windward streamline laminar solution is obtained for the body, with the heating rate distribution off the streamline calculated from an empirically derived correlation. By assuming that the boundary layer growth in turbulent flow is affected to the same order by angle of attack as it is for laminar flow, the turbulent heating rate ratio to a stagnation point on a one-foot hemisphere nose cap can be estimated. In regions of separated flow which are assumed to exist on the surfaces shadowed by the velocity fields, another empirical correlation is used.

E.2 STAGNATION POINT HEATING RATE SOLUTION

The stagnation point real gas heating rate to a one-foot radius sphere for each exhaust plume will be estimated as outlined in Reference E-1.

Either the real gas input transport properties or those calculated by the simplified equations within the subroutine are used in conjunction with the following stagnation point heating rate equation. This equation has been empirically derived for arbitrary high enthalpy gas mixtures.

$$q_{sp} = \frac{Nu}{\sqrt{Re}} \sqrt{\rho_L \mu_L} \frac{1.8}{Pr} (H_s - H_w) \sqrt{\frac{dV}{dS}} \quad (E.1)$$

where

$$\frac{Nu}{\sqrt{Re}} = \left[\frac{Pr}{Pr_w} \sqrt{\frac{T_L \mu_w}{T_w \mu}} \right] \left[1 - \frac{H_w}{H} \right]^{1.15}$$

This determination for the plume gas stagnation point heating rate is then used with the local-to-stagnation heating rate distribution q_L/q_{sp} (laminar and turbulent) to give an absolute heating rate to each segment of the body configuration.

E.3 WINDWARD STREAMLINE HEATING DISTRIBUTION (q_L/q_{sp})

E.3.1 Angle of Attack Above 50°

When the body is oriented at angles of attack greater than 50° to the flow field, heating rates to the cone frustum and/or cylinder portion of the configuration have been programmed as:

$$q_L/q_{sp} = \sqrt{\frac{1}{2}} \left[\cos^{1.2}(\delta) \right] \left[\frac{1}{\sqrt{R_c \mu}} \right] \quad (E.2)$$

The variables δ and R are evaluated in the following manner:

Cylinder: δ = angle of attack
 R_c = radius of cylinder

Cone: δ = cone half angle plus angle of attack
 R_c = $\gamma \cos \theta_c$ where γ = radial coordinate of cone and θ_c = the cone half angle

Hemisphere: For the hemisphere at angles of attack, the heating rate distribution is calculated similarly to zero angle of attack

E.3.2 Angle of Attack Below 50°

For lower angles of attack, a solution of heating rate distribution has been programmed in a manner which permits a boundary layer growth to be determined over the composite body shape which is being analyzed. The fundamental heating rate ratio for laminar flow is given as

$$q_L/q_{sp} = .332/q_{sp}(\rho^* \mu^*)^{1/2} (V_L)^{1/2} (Pr^*)^{-2/3} \frac{1}{(X_{sf})^{1/2}} (H_{aw} - H_w) \quad (E.3)$$

This equation is basically the Blasius flat plate equation as modified by Eckert (Reference E-2) for compressible flow and by Vaglio-Laurin (Reference E-3) for the existence of pressure gradients normal to the local streamlines over the windward surface of a body. This modification is primarily a coordinate transform which makes use of the pseudo-boundary layer growth length so that the ordinary flat plate heating equation may be used to predict the heating distribution over the windward surfaces with curvature when the body is at low (0 to 50°) angle of attack.

Although this method may be applied to the entire surface to be analyzed, the extent of this effort limits its use to the laminar windward streamline of axisymmetric shapes at angle of attack. As stated earlier, empirical correlations are used to determine heating rates off this streamline. However, by determining this windward streamline distribution by an exact method, the distributions off the streamline are most realistic.

The primary objective in this type of analysis is to evaluate a pseudo-characteristic length (X_{sf}) for use in the modified flat plate equation in Equation (E.3) as the boundary layer grows over the body being analyzed. As stated in References E-2 and E-3, the characteristic length is:

$$X_{sf} = \frac{1}{\rho^* \mu^* V_L r^2} \int_{s_i}^{s_f} \rho^* \mu^* V_L r^2 dS + X_{si} \quad (E.4)$$

E-3

Since the governing equations become even more complex when a similar analysis is made for turbulent flow, the assumption that the pressure gradient causes the same growth characteristics to a turbulent boundary layer is made. The inherent differences between laminar and turbulent zero angle of attack axisymmetric solutions are extended to solutions for non-zero angle of attack in this analysis. This assumed variation between the included exact laminar heating rate solution and the to-be-calculated turbulent heating rates gives an estimate of the turbulent boundary layer growth. This assumption is valid within the order of previous assumptions made for this estimated plume convective heating subroutine. A transition criterion of Re_θ over M_L ratio has been chosen as the mechanism for changing from a laminar to a turbulent heating rate calculation. The fundamental turbulent heating rate equation is similar to the one used for the laminar case and is

$$q/q_{sp} = \frac{.0296}{q_{sp}} \frac{(\rho^* V)^8 (\mu^*)^{-.2}}{Pr^{.666}} (H_{aw} - H_w) \frac{1}{X_{sf}^{.2}} \quad (E.5)$$

Note that the parameter X_{sf} appears in both Equations (E.3) and (E.5). This characteristic length has been analytically evaluated. The results of this evaluation are listed in Tables E-1 and E-2. As can be seen from these tables, the logic going from one set of equations to another depends primarily on the segment analyzed immediately before the segment to be analyzed, and upon any expansion, compression, or body discontinuities encountered as the analysis moves from one segment to the next.

E.4 ORDER OF SOLUTION

A general body shape is shown in Figure E-1. The general configuration can be described as a series of conic sections with subsections. Integration for determining the pseudo-characteristic length (X_{sf}) over each subsection on the windward streamline has a variety of start conditions which determines the type of solution for the windward heating analysis. These beginning boundary layer parameters or initial conditions for each subsection are described in the following paragraph. A listing of equations used to calculate the characteristic length for each of the various configurations is given in Table E-2. As can be seen, the calculation of the windward streamline heating rates is an

Table E-1

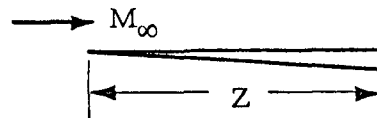
| Conic Section | s_f | X_{sf} | $X_f = X_i + \Delta X$ |
|------------------|---|---|---|
| General Equation | | | $X_{sf} - X_{si} = \frac{1 \int_{s_i}^{s_f} \rho^* \mu V_L^2 r^2 ds}{\rho^* \mu V_L^2 r^2}$ |
| Flat Plate | $s_f = X_f$ | | $X_{sf} = \Delta X + X_i$ |
| Cone | $s_f = s_i \left[e^{(\cos^2 \theta_c + A)} + \frac{X_f}{X_i} \right]$ | $X_{sf} = \mu^* \rho^* V_L^2 s_i^2 \left[e^{2(\cos^2 \theta_c + A)} (X_f - X_i) \right. \\ \left. + \left(e^{(\cos^2 \theta_c + A)} \right) \left(\frac{X_f^2}{X_i} - X_i + \frac{1}{3} \frac{X_f^3}{X_i^3} - X_i \right) \right] + X_{si}$ <p>where</p> $A = \frac{\cos^2 \theta_c}{\sin \theta_c} \frac{49}{V_L} \left(\frac{2}{\gamma} T \right)^{1/2} \left(\frac{P}{1 - P_L} \right)^{1/2}$ | |
| Cylinder | $s_f = s_i e^{\left[\frac{49}{V_L Re} \left(\frac{2}{\gamma} T_L \right)^{1/2} \left(\frac{P}{1 - P_L} \right) (X_f - X_i) \right]}$ | $X_{sf} = K \frac{F(X_f - X_i)}{F} - \frac{1}{F}$ <p>where</p> $K = \mu^* \rho^* V_L^2 s_i^2$ $F = \frac{98}{V_L Re} \left(\frac{2}{\gamma} T_L \right)^{1/2} \left(\frac{P}{1 - P_L} \right)^{1/2}$ | |

Table E-2

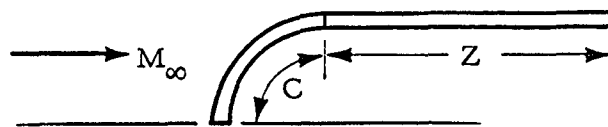
| Segment Type Preceding | s_i | X_{si} | X_i |
|------------------------|--|--|--|
| A | $s_i = s_f$ | $X_{si} = X_{sf}$ | $X_i = X_f$ |
| B | $s_i = 0$ | $X_{si} = 0$ | $X_i = 0$ |
| C | $s_i = Re \sin(\theta - \alpha)$ | $X_{si} = \frac{(.332)^2}{2} \frac{(\rho^* \mu^* V_L)}{q_L (Pr^*)^{4/3}}$ | $X_i = X_{si}$ |
| D | $s_i = \left[X_{si} \left(\frac{2A+1}{K} \right) \right]^{\frac{A}{(2A+1)}}$ | $X_{si} = \left(\frac{P_{LD}}{P_{LZ}} \right)^2 \left(\frac{V_{LD}}{V_{LZ}} \right)^3 \left(\frac{\mu_D^*}{\mu_Z^*} \right) \left(\frac{\rho_Z^*}{\rho_D^*} \right) X_{sfD}$ | Cone |
| | | | $X_i = \left[\left(\frac{2A+1}{K} \right) X_{si} \right]^{\frac{1}{(2A+1)}}$ |
| E | $s_i = \left[X_{si} \left(\frac{2A+1}{K} \right) \right]^{\frac{A}{(2A+1)}}$ | $X_{si} = \left(\frac{V_{LE}}{V_{LZ}} \right) \left(\frac{\mu_E^*}{\mu_Z^*} \right) \left(\frac{\rho_Z^*}{\rho_E^*} \right) X_{sfD}$ | Cylinder |
| | | | $X_i = \ln \left(\frac{2FX_{si}}{K} \right)^{\frac{1}{2A}}$ |



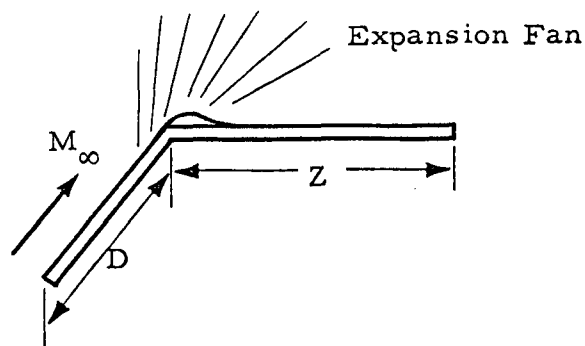
(a) Segment is a Conic Section



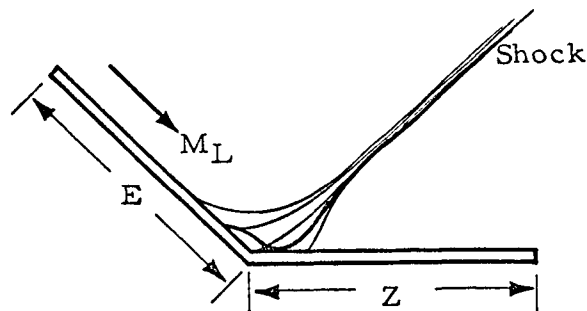
(b) No Segment (leading edge or sharp point)



(c) Hemisphere Nosecap



(d) Segment Creating an Expansion Corner



(e) Segment Creating a Compression Corner

Figure E-1 - General Body Configuration

integral procedure which must begin at the stagnation point. The growth of the boundary layer is then traced over the vehicle as it changes shape and passes through various expansion and compression corners and finally ends at the last body station of the body under analysis.

Included herein are the basic sections and their initial conditions as they are analyzed by this program. When given a segment of windward streamline on any conic section with the preceding streamline segment given as A, B, C, D, or E, we may have the following configurations leading to different initial conditions in the evaluation of the heating rate characteristic length to segment Z. By placing the various assorted segments end to end, the boundary layer growth and consequent heating rate may be traced step-wise down the body from section to section.

E.5 START CONDITIONS

The values of S_i and X_{si} (Equation (E.4)) must be chosen to start the integration down the most windward streamline for each time step and consequent analysis of heating distribution. If the first section is sharp-edged, the parameters become equal to zero. If the body is capped by a blunt nose cap, the values of X_{si} and S_i are obtained by using the heating rate as predicted by Reference E-4 to analytically find the correct X_{si} and S_i for the start conditions of the integration. Table E-2 shows the initial conditions for the integration over each conic section which must be used to find a heating rate at the end of each following section.

E.6 CYLINDER AND CONE INTEGRATIONS

Determination of X_{si} and S_i has been made for both the cone frustum and the cylinder conic section. The analytic solution for their values is listed in Table E-2. These relationships are programmed so that the heating rate may be evaluated at each station down the body. No programmed integrations were necessary due to the analytic solution of the conic cylinder sections. Once this laminar boundary layer growth characteristic X_i is determined, it is assumed that the boundary layer growth of the vehicle being at angle of attack is similar for the turbulent heating distribution. From this assumption, the characteristic length for turbulent flow is assumed to be the laminar characteristic

growth length multiplied by a factor determined by the Mangler transformation (Reference E-5) for the cone and by a factor of 1 for the cylinder. The analytic solution for the integration for laminar flow is shown with the cone and cylinder conic sections in Table E-2.

E.7 DISCONTINUITIES

With the varied combinations of nosecone and/or cylinder configurations, both compression and expansion corners will be encountered throughout the integration. These discontinuities in the X_{si} and S_i determination must then be adjusted to give a true boundary layer growth length after moving through an expansion fan or compression shock. In reference to Figure E-1, the modified values for the initial conditions of X_{si} and S_i in the following segment integration are listed in Table E-2. The method as outlined in Reference E-6 was used to obtain these expressions. This method is primarily an analytic momentum thickness boundary layer match as the flow moves from one region to the next.

E.8 LOCAL PROPERTIES

The local flow properties are obtained from the main method of characteristics program. The reference transport properties are evaluated by the Eckert reference temperature method and are calculated by the following equations taken from Reference E-6.

$$\mu = 2.27 \times 10^{-8} \frac{T^{*3/2}}{T^* + 198.72} \sim \frac{\text{lb-sec}}{\text{ft}^2} \quad (\text{E.6})$$

$$K = 3.172 \times 10^{-7} \frac{T^{*3/2}}{\left(T^* + 441.72 \left(e^{-\frac{49.73}{T^*}}\right)\right)} \frac{\text{Btu-ft}}{\text{ft}^2 \text{-sec}^\circ \text{R}} \quad (\text{E.7})$$

These relationships are necessary for getting a distribution of heating rates over the bodies. However, since the heating rates are ratioed, any effects due to the equilibrium gas assumption will be nullified as the stagnation point heating

rates are ratioed to the distribution heating rates. It becomes necessary only to accurately obtain the stagnation point heating rate. The programmer decides whether to use (1) the included property transport equations or (2) input values for the stagnation point conductivity, viscosity and specific heat.

E.9 OFF-WINDWARD STREAMLINE DISTRIBUTION

E.9.1 Greater Than 50° Angle of Attack

The heating rate off the windward streamline is calculated by application of the distribution about yawed cylinders, as described in Reference E-4. As a local deflection angle becomes less than zero degrees (shadowed flow) the flow is assumed to separate, and the local heating rates to the leeward surface are calculated as described in the separated flow discussion.

E.9.2 Less Than 50° Angle of Attack

The heating rate off the windward streamline for angles of attack less than 50° is calculated by adjusting the characteristic length to include the additional growth of the boundary layer as it transverses a greater length of the body. This adjustment is a geometry change that is represented by the equation

$$X_{sf_0} = X_{sf} \left(\frac{X}{Re} \right) . \quad (E.8)$$

This characteristic length is used with the same laminar or turbulent flat plate heating equations (E-3 and E-5) as were used for calculation of the windward streamline heating rates.

E.10 SEPARATION

The following empirical relation was used to determine separation heating rates to body locations on the leeward side of the configuration under analysis. This empirical correlation has been stated previously primarily for laminar flow heating rate predictions. It was beyond the scope of this

effort to determine similar heating rate method for turbulent flow. As can be seen in the equation, the local deflection angle of the section under consideration is a primary driving factor when separated flow on the shadowed side of the configuration is considered. A characteristic length based on the distance from the separation point is a secondary parameter.

$$\frac{q_L}{q_{\text{prior to separation}}} = \frac{1}{e^{.6\Delta\delta}} \left(\frac{X_{si_{\text{prior to separation}}}}{X_{si_{\text{prior to separation}}} + l} \right)^{\frac{1}{2}} \quad (\text{E.9})$$

where

- l is geometric shortest distance to local separated point
- $\Delta\delta$ is local flow angle to surface angle difference

E.11 CONCLUSION

In conclusion, the convective heating subroutine presented in this Appendix contains analytic heating rate solutions for the windward streamline of axisymmetric shapes, as well as engineering approximations for heating rates off this streamline. These solutions are based on a streamline divergence technique which includes the use of real gas local flow properties supplied by the method of characteristics program. Judicious application of these methods will produce satisfactory heating rate distributions over a great variety of axisymmetric configurations immersed in rocket exhaust flow fields. However, it should be realized that the heating rate prediction techniques off the most windward streamline are only engineering approximations and further work is required before rigorous analytic solutions will be available.

APPENDIX E REFERENCES

- E-1 Marvin, Joseph G. and George S. Deiwert, "Convective Heat Transfer in Planetary Gases," Ames Research Center, Moffett Field, California, NASA TR R-224, July 1965.
- E-2 Eckert, E. R. G., "Survey of Boundary Layer Heat Transfer at High Velocities and High Temperatures WADC Technical Rpt. 59-624, April 1960.
- E-3 Vaglio-Laurin, Roberto, "Turbulent Heat Transfer on Blunt-Nosed Bodies in Two-Dimensional and General Three-Dimensional Hypersonic Flow," J. Aerospace Sci., January 1960.
- E-4 Lees, Lester, "Laminar Heat Transfer Over Blunt-Nosed Bodies at Hypersonic Flight Speeds," Jet Propulsion, Vol. 26, No. 4, pp. 249-269, Apr. 1956.
- E-5 Mangler, W., Boundary Layers on Bodies of Revolution, AVA Rpt. 45/AD17, 1945.
- E-6 Brown, E. A., "Aerodynamic Heat Transfer Handbook, Vol. I," D2/9514, 5 March 1961.